Barcelona Mobile World Congress

Mobile Communications 2011

A Special Supplement to Microwave Journal

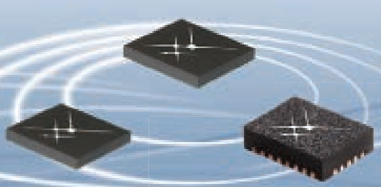

SKYWORKS®

Antenna Switches: Discretes and Modules

For 3G/4G Wireless Broadband and Mobile Handset Applications

Part Number / Description	Linear TRx Ports	Rx Ports	Rx SAW	Typ. IL TRx/Tx @ 2.0 GHz (dB)	Typ. Isolation (dB)	IMD (dBm)	H2/H3 Typ. (dBm)	Package (mm)
SP8T–SP10T Antenna Switch Modules—With GSM Harmonic Filter								
SKY18106-455LF SP8T, SPI DigRF interface	6	0	No	-0.6/-0.9	-30	-106	-50/-45	QFN 26L 3.0 x 3.8
SKY18110 SP8T, GPIO logic	6	0	No	-0.8/-0.9	>35	<-102	-45/-42	MCM 20L 3.2 x 3.2
SKY18116 SP8T, small form factor	6	0	No	-0.8/-0.9	>35	<-102	-45/-42	MCM 18L 3.2 x 2.5
SKY18108 SP9T, WCDMA, and TD-SCDMA	3	4	No	-0.8/-0.9	>35	<-102	-45/-42	MCM 20L 3.2 x 2.5
SKY18120 SP9T, WCDMA, and TD-SCDMA	3	4	No	-0.8/-0.9	>35	<-102	-45/-42	MCM 16L 2.5 x 2.5
SKY13364-389LF SP10T	4	4	No	-0.6/-1.0	>35	<-105	-40/-40	QFN 26L 3.0 x 3.8
SKY13362-389LF SP10T	5	3	No	-0.7/-1.1	>35	<-105	-40/-40	QFN 26L 3.0 x 3.8
SKY13402-466LF SP10T	6	2	No	-0.7/-1.1	>35	<-105	-48/-42	QFN 26L 2.6 x 3.4

Part Number / Description	Linear TRx Ports	GSM Rx Ports	GSM Harmonic Filter	GSM Rx Band SAW Filter	Typ. IL TRx/Tx @ 2.0 GHz (dB)	Typ. Isolation (dB)	IMD (dBm)	H2/H3 Typ. (dBm)	1.8 V Logic Compatible	Package (mm)
SP2T–SP6T Rx Diversity, Band, Mode Switch, and Differential Rx Switch										
SKY13374-397LF SP2T	2	–	–	No	0.5	>28	–	-50/-50	–	QFN 16L 2.0 x 2.0
SKY13373-460LF SP3T	3	–	–	No	0.5	>23	–	-50/-50	–	QFN 12L 2.0 x 2.0
SKY13388-465LF SP4T	4	–	No	No	0.5	>25	–	-45/-45	Yes	QFN 12L 2.0 x 2.0
SKY13380-350LF SP4T	4	–	–	No	0.4	>23	<-115	-45/-45	–	QFN 16L 3.0 x 3.0
SKY13358-388LF SP5T	5	–	–	No	0.7	>27	<-102	-50/-45	–	QFN 16L 2.3 x 2.3
SKY13360-388LF SP6T	6	–	No	No	0.5	>23	< 100	-40/-40	Yes	QFN 16L 2.3 x 2.3
SKY13354-368LF DP4T	0	2	No	No	0.5	> 23	–	–	No	QFN 12L 2.0 x 2.0
SKY13397-388LF DP5T, 3G band switch	5	–	–	No	0.4	>32	–	-50/-50	–	QFN 16L 2.3. x 2.3

Skyworks Green™ products are compliant to all applicable materials legislation and are halogen-free. For additional information, refer to Skyworks Definition of Green™, document number SQ04-0074.

For more information on our broad product portfolio, visit our Web site at www.skyworksinc.com

USA: 781-376-3000 • Asia: 886-2-2735 0399 • Europe: 33 (0)1 43548540 • Email: sales@skyworksinc.com
www.skyworksinc.com • NASDAQ: SWKS

Table of Contents

Staff

Publisher: Carl Sheffres
Editor: David Vye
Managing Editor: Jennifer DiMarco
Technical Editor: Patrick Hindle
Associate Technical Editor: Dan Massé
Staff Editor: Kerri Germani
Editorial Assistant: Barbara Walsh
Consulting Editor: Harlan Howe, Jr.
Consulting Editor: Frank Bashore
Consulting Editor: Peter Staecker
Consulting Editor: Dan Swanson

Web Editor: Chris Stanfa
Audience Development Manager: Michelle Barry
Traffic Manager: Edward Kiessling
Marketing and Event Coordinator: Kristen Anderson
Director of Production & Distribution: Robert Bass
Lead Designer & Production Coordinator: Janice Levenson
Graphic Designer: Sachiko Stiglitz

EUROPE

International Editor: Richard Mumford
Office Manager: Nina Plesu

CORPORATE STAFF

CEO: William M. Bazzy
President: Ivar Bazzy
Vice President: Jared Bazzy

Attending Mobile World Congress

David Vye, Microwave Journal *Editor*

For the cover of this month's Mobile Communications supplement, we found artistic inspiration from one-time Barcelona resident Pablo Picasso in our tribute to the city's other famous resident – GSMA Mobile World Congress (MWC). This annual event combines the world's largest exhibition for the mobile industry and gathering of Chief Executives and other dignitaries from up and down the global mobile supply chain. And in 2012, Barcelona has even more reason to celebrate the return of MWC.

MWC, initially called 3GSM when it started in 1987, was hosted in Cannes until 2006 after which it moved to Barcelona. Over the past few years, rumors of a new location have been spreading throughout the exhibition halls as the organizers put the show out to bid. In considering a possible new venue, GSMA undertook a thorough and complex evaluation process, starting with 30 cities, narrowing it down to six before reducing the number of candidates down to a short list of four finalists. Cities such as Munich, Milan and Paris aggressively vied for the opportunity to host the event. But then in July, after an 18-month search, the GSMA announced that Barcelona had been selected as the "Mobile World Capital" from 2012 to 2018.

As the Mobile World Capital, Barcelona will remain as the host of the industry's largest yearly event. The cornerstone of the Mobile World Capital is the four-day MWC, which attracted more than 60,000 attendees from 200 countries in 2011. Attendees included 3000 CEOs, government delegations from 131 countries and more than 2900 media representatives. Starting in 2013, the MWC will be relocated within the city to the cutting-edge venue Fira de Barcelona Gran Via.

In addition to MWC, the Mobile World Capital features two additional elements: the Mobile World Centre and the Mobile World Festival. The Mobile World Centre will be composed of permanent and temporary exhibitions that meld culture and technological innovation, facilities for the development and incubation of mobile solutions, and retail and hospitality venues. The Mobile World Festival, which is targeted to the general public, will incorporate a range of activities, including sporting events, music and art festivals, film awards, applications and technology fairs and more.

According to estimates from the Barcelona Candidacy, the Mobile World Capital would bring, in the first year alone, more than 300 million euro, along with thousands of part-time jobs. As some of the initiatives have a mid-term reach and will grow steadily during their implementation, the economic impact is expected to increase progressively and, based on Barcelona's assessments, could reach 3.5 billion euro over the seven years.

(Continued on page 5)

As for MWC 2012, the keynote speakers are once again C-level telecommunication executives representing the top of the food chain. Network CEOs from AT&T, Alcatel-Lucent, Deutsche Telekom, NTT DOCOMO, Vodafone, Ericsson and Telecom Italia will join CEOs from major handset OEMs, such as Nokia and HTC, to discuss the future direction and immediate concerns of the industry. Some of the focus sessions will examine mobile innovations, strategies, addressing network capacity, regional focus and network technology evolution.

From the RF/microwave component sector, companies participating at MWC are particularly active in the commercial communications side of test and measurement equipment, semiconductor and chipsets, cables/connector and high power passive components, antennas, femto-cells and backhaul equipment manufacturing. On the test and measurement side, we are anticipating major product announcements from companies such as Aeroflex, Agilent, Anritsu, Rohde & Schwarz and Spirent. RFIC manufacturers, such as TriQuint Semiconductor, RFMD, Skyworks, ANADIGICS and Avago, will most likely show up with a hail of new products as well.

In this month's special mobile communications supplement, we are pleased to have Fred Schindler, Director of RFMD's Boston Design Center, and his colleagues discuss how power amplifier design is impacted by the higher data rates and linearity requirements called for by LTE. This is no small challenge for the RFIC designer and should be of considerable interest to anyone working with a mobile device front-end.

Complementing this cover story, we are also featuring a perspective piece from Ron Williamson of Aeroflex Test Solutions on the future of RFIC test strategies. Williamson talks about the growing cost and equipment investment for RFIC ATE systems and how PXI/AXIe instrumentation and infrastructure offer an alternative production test environment with the benefit of high MTBF, fast test times and system coherency. Also discussing test issues for mobile communications, Agilent Technologies writes about the design and test challenges for the physical layer of base station and user equipment brought on by the carrier aggregation called for by ITU's IMT-Advanced 4G.

Along with articles on the co-existence of point-to-point microwave links, the design of a compact MIMO antenna using metamaterials, addressing traffic and channel power distribution, low PIM connectors and GPS ICs, *Microwave Journal* covers a lot of ground in this month's supplement, not unlike the new Mobile World Capital. So here is to Barcelona and MWC. I am glad mobile decided to be stationary. ■

MOBILE. WORLDCONGRESS

Mobile World Congress

February 27-March 1, 2012
Barcelona, Spain
For more information, visit
www.mobileworldcongress.com

Wireless Data Connectivity with LTE Power Amplifiers

Consumers are demanding more from their mobile devices – including increased bandwidth. They have become accustomed to the near universal data connectivity of smartphones, and are voracious for the applications that continually demand higher and higher data rates. Tablet computers also are becoming more popular, and their demands for constant connectivity and data usage are reportedly five times higher than those of smartphones.[1] Laptops have not disappeared either. Consumers expect their laptops to have the same universal connectivity as their phones, running applications that demand higher data rates. Most laptops have wireless network connectivity built-in, and there is a growing market for USB dongles to provide connectivity with the latest high data rate standards. There is also an emerging market for new categories of connected devices, ranging from Internet Protocol TV (IPTV) to connected vehicles with wireless diagnostic, safety and infotainment capabilities.

What is driving these increased data rates? In the US, for example, the introduction of advanced smartphones is pushing some networks to their limits and frustrating consumers. We have all seen the growth of streaming audio and video, and this is just the tip of the iceberg. The exponential growth of social networking-related traffic is another key driver, as is online gaming. Perhaps the most compelling trend is the growth of cloud computing. With cloud computing, data is stored remotely, not on the device. As we have all seen, the amount of data that we want to store continues to increase. More data can be stored in the cloud than can be practically stored on a mobile device. Reducing the permanent memory demands in the mobile device reduces cost and size and increases speed and battery life. Thus, we have a hardware trade-off between permanent memory and network connectivity. The balance is tipping in the direction of data connectivity.

Mobile data traffic increased by a factor of 2.6 in 2010, and is expected to increase 26 fold from 2010 to 2015.[1] By the end of this year, it is expected that video will be more than 50 percent of all mobile traffic. In fact, in the US we have already seen streaming video services like Netflix dominating Internet traffic at peak times.[2] Consumers are migrating to mobile devices and that is driving mobile traffic.

In order to support this growing demand, connection speeds are expected to increase by a factor of ten by 2015. Today, the average mobile network connection worldwide is only 215 kbps. By 2015, it will be more than 10 times that, 2.2 Mbps. With 7.1 billion mobile connected devices, that is a lot of data.[1] Network

Fred Schindler, Virender Sadhir, Brian Robbins, David Guo and Jerry Paradis
RF Micro Devices, Greensboro, NC, and Billerica, MA

infrastructure is already responding to meet the challenge. Long Term Evolution (LTE) and LTE-Advanced have been developed specifically to provide high mobile data capacity.

LTE CONNECTIVITY

Connections to LTE networks are already available from various cellular service providers in limited service areas. These deployments continue to grow. But there are other LTE deployment options. For example, in-home range extenders can be used to provide enhanced connectivity, especially in rural or remote areas. Personal gateways will also find use, primarily by businesses, to provide higher data rates either in office facilities or in public service areas to provide an enhanced experience for customers, much as many cafés offer free WiFi today.

There are of course alternatives to LTE. WiFi is a leading alternative, and currently can offer connection speeds of 300 Mbps. Future variants on the 802.11 standard will offer even higher data rates. WiFi is pervasive and offers an attractive option to connect to a local access point, typically with a range of tens of meters. WiFi uses either the 2.4 to 2.5 GHz ISM band or the 4.9 to 5.85 GHz band (4.9 to 5.15 GHz in Japan). The ISM band is crowded – it is used for a variety of other data connections, including Bluetooth® and microwave ovens. This ultimately limits the practical achievable data rate. The 5 GHz band is an attractive alternative, but many devices lack 5 GHz capability and the band remains lightly used.

WiMAX is another alternative. It was designed with many of the same applications in mind as LTE, and is approximately equivalent in capability. WiMAX has been deployed in the 2.3 to 2.4 GHz, 2.5 to 2.7 GHz and 3.3 to 3.8 GHz bands, but it has seen limited acceptance in the marketplace. LTE can also use these frequency bands and many WiMAX compatible uplink products (such as datacards) can be redesigned to operate in high data rate LTE systems. Future migration trends point to growing adoption of the LTE standard.

LTE operates in a variety of bands between 728 MHz and 3.8 GHz, depending on the service provider and the location. Bandwidths, data rates, and TDD/FDD implementation vary, but the overall standard is universal. Data rates of up to 300 Mbps are possible for LTE and 3.3 Gbps for LTE Advanced (though this is only under ideal conditions with 8 × 8 MIMO). One of the main advantages of LTE is that it has been selected as the 4G standard by a large number of cellular service providers throughout the world.

UPLINK VS. DOWNLINK

Every wireless system has an uplink and a downlink. Typically, we carry a terminal device (smartphone, tablet, laptop or other connected device). The devices connect to an access point or a base station, see ***Figure 1***. The downlink is from the access point to the networked device. Conversely, the uplink is from the network device to the access point. Typically, the devices we carry download more data than they upload. In this article, we are highlighting power amplifiers because they are a critical component in the system. The requirements for uplink and downlink power amplifiers are very different.

Downlink power amplifiers are found in access points and base stations and are used to transfer data to various mobile devices. An access point must connect to multiple network devices simultaneously, multiplying the total data rate, so power and linearity requirements for the downlink are tougher than for an uplink. For LTE, linearity is measured as Adjacent Channel Leakage Ratio (ACLR),[3,4] which is similar to the ACPR measurement used for CDMA and W-CDMA. LTE linearity is typically required to be -44 dBc for the downlink, usually targeting an OFDMA waveform for the greatest data rate, with bandwidths of 10 to 20 MHz (up to 100 MHz for LTE Advanced).

Uplink power amplifiers are found in smartphones, USB dongles, laptops, tablets, IPTVs, connected automobiles, etc. Each device provides its own uplink so the requirements on power and linearity are less stringent. System ACLR is typically -35 dBc with a 10 MHz standard bandwidth.

In LTE, modulation also differs from uplink to downlink. In the uplink, a single carrier frequency division multiple access (SC-FDMA) modulation is used. The downlink, in contrast, uses orthogonal frequency division multiple access (OFDMA).

▲ *Fig. 1 A networked device uses an uplink and a downlink.*

Whereas SC-FDMA uses a single carrier, OFDMA uses multiple orthogonal carriers. This provides greater spectral efficiency for the downlink, but challenges PA linearity even more.

ACLR is not the only linearity requirement for an LTE PA. There is also a requirement for error vector magnitude (EVM). For the LTE downlink, depending on the specifics of the modulation, the EVM limits are 12.5 to 17.5 percent.[4] As a practical matter, the ACLR limit of -44 dBc is always reached long before EVM approaches 10 percent, so EVM is not a significant PA design concern. Other systems, such as WiMAX and WiFi tend to be EVM limited, with EVM specifications in the 3 to 4 percent range.

LINEARITY AND MODULATION BANDWIDTH

As systems are designed to provide even higher data rates, the linearity requirements inevitably continue to increase. And, as air standards evolve to handle greater bandwidths and modulation techniques become more advanced, the general trend is for greater linearity burden on the power amplifier.

LTE supports a range of modulation bandwidths. For an uplink, the modulation bandwidth may be 1.4, 3, 5, 10, 15 or 20 MHz. For the downlink, the standard modulation bandwidths are 10 and 20 MHz. The standard WiMAX downlink modulation bandwidth is 10 MHz, optionally 20 MHz (LTE-Advanced supports up to a 100 MHz modulation bandwidth). In addition to linearity challenges, the modulation bandwidths themselves create design challenges for a PA.

DESIGNING PAS FOR NETWORK ACCESS POINTS

As already noted, system linearity is stated in terms of ACLR. The downlink power amplifier must be capable of -44 dBc ACLR or better, up to its rated power. Rated power for the PA is dependent on a number of factors. First, consider the type of access point. See ***Table 1*** for a listing of access point types. A macrocell is what we typically think of as a base station – a tower servicing a large geographic area. A microcell is a base station that services a more limited area, often in an urban area, with denser cell spacing allowing for increased network capacity. A picocell covers an even smaller area, often a specific office facility, mall, or sporting complex. A femtocell is smaller yet, and is typically intended to service a home or small business. Picocells and femtocells will be deployed to offload high data traffic onto local fixed network connections.[1]

TABLE I

CHARACTERISTICS OF ACCESS POINT TYPES

Access Point Type	*Typical Range*	*Output Power at the Antenna*
Femtocell	10 to 50 meters	10 to 25 dBm
Picocell	Up to 200 meters	22 to 30 dBm
Microcell	Up to 2 km	1s to 10s of watts
Macrocell	Up to 30 km	10s to 100s of watts

We need to work back from the output power at the antenna to determine the requirements for our power amplifiers. In a Time Division Duplex (TDD) system, we typically see 1.5 to 2 dB of loss from switching and filtering between the PA and the antenna. A Frequency Division Duplex (FDD) system requires additional filtering, so the loss between the PA and the antenna is higher, 2.5 to 3 dB. There is a range of power requirements for every access point type, but there is a typical requirement that satisfies most implementations. We have found that power outputs in the 23 to 26 dBm range satisfy most femtocell and some picocell requirements.

KEY PA DESIGN CONSIDERATIONS

One of the first steps in designing a PA is process selection. The best design philosophy is always to pick the process that best fits the full set of requirements. Forcing a non-optimal process on an application will almost always yield an inferior product in terms of performance and/or cost. A fundamental choice is between Si and GaAs. For an access point downlink, performance is very important. There has been considerable progress in CMOS and SiGe power amplifiers, but up to now performance has typically lagged GaAs. In addition to a performance advantage, GaAs typically offers much shorter development times, thereby quickening time to market.

Within the family of GaAs processes, there are many options. HBTs and PHEMTs can both provide excellent PA performance. HBTs have an advantage in size, ease of matching and bias, so are a logical choice. There are a number of HBT processes available, and of those, InGaP shows a modest advantage for linear PAs. So an InGaP HBT is a good process to choose for an LTE downlink PA. GaAs BiFET can also be attractive – BiFET offers HBTs and PHEMTs on the same die. This makes it easy to integrate control functions, switches and receive circuitry. We are interested in a PA without switching or a receive path, and only modest control functionality is required. So the added complexity of a BiFET process is not necessary.

Once the transistor and process have been selected, it is time to architect the PA. The first priority is to determine how many stages of amplification are needed. We know that 30 dB gain is adequate for the vast majority of applications. While this can be achieved with two stages, three stages are preferable. It is generally necessary to sacrifice some gain to meet the wide range of other requirements – linearity, input and output match, bandwidth, passband flatness, temperature, process variation, stability, and harmonic output levels are just some of the additional specifications that need to be met. The extra gain of an added stage avoids over constraining the design. Current consumption is also a key requirement and an added stage does increase the total current draw. But the

increased transistor area from the added stage can be modest, so with careful bias design the impact on total power consumption is minimal.

Sizing transistors is also critical. We start with the output, which must be large enough to provide the necessary combination of power and linearity. It must also be large enough to ensure that power density and temperature do not exceed reliable limits. We can rely on load-pull characterization of the transistors, as well as past experience of what is necessary for a certain level of output power.

While uplink PAs are typically powered by a battery (2.7 to 4.8 V), downlink PAs are typically powered by a fixed supply (4.5 to 5.0 V). It has been determined that 1900 μm^2 of emitter area is about right for the output stage of picocell to femtocell downlink PA delivering 22 dBm of linear power. Having determined the size of the output stage, we can determine the area of the other stages. The output stage will deliver about 8 dB gain, so the first and second stages will deliver about 11 dB each. We need to ensure that the earlier stages do not limit linearity. To do this with adequate margin over all conditions, we choose a 4:1 transistor size ratio between stages. Our final transistor configuration is 120, 480 and 1920 μm^2.

Now that we have selected the transistors, we have to determine how to best bias them. The simplest and physically smallest is to have a common bias path for all three stages, as ***Figure 2a*** shows. In such an approach, transistors in all three stages are biased at the same operating point, running at the same current density. An alternative is shown in ***Figure 2b***. This allows us to adjust the operating point, or current density for each stage. There are significant benefits to using this method. The output transistors should be the only ones limiting linearity, so their bias points should be set with that in mind. Similarly, the input stage is primarily providing gain, which can best be done at a different operating point. Finally, current consumption at each stage can be set to the minimum necessary for each, minimizing total current draw.

Also related to bias is thermal management. The duty cycle of an LTE downlink signal is high and with a long duration, so from a thermal management perspective, we can consider it to be CW. Once the power dissipation has been determined, the PA needs to be laid out for reliable operation, with particular emphasis on the transistor layouts. A PA in a picocell or a femtocell needs to operate in an ambient temperature of up to 80°C.

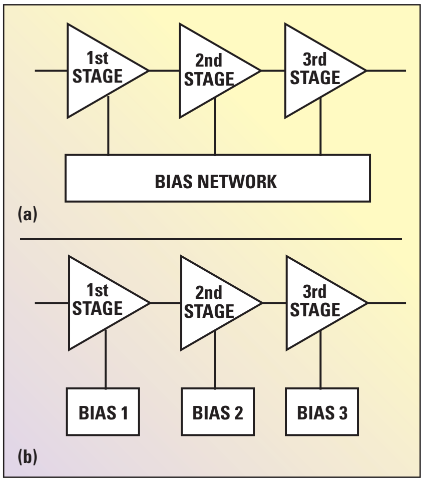

▲ *Fig. 2 Two approaches to biasing a multi-stage PA (a) common bias for all stages and (b) individual bias for each stage.*

The next critical step is matching. For many PA applications, it is important to determine the optimal match for linearity for the output transistor. For an LTE downlink PA, it is best to use an optimal power match. Because the LTE downlink uses OFDMA, it has a peak to average power ratio of about 10 dB.[5] The result is seen in ***Figure 3***. ACLR starts to increase significantly above an output power of about 21 dBm. This is about 10 dB below the level where output power starts to compress heavily. Peaks in power 10 dB above the average cause the limiting nonlinearities. A similar effect can be found in an LTE uplink PA, but because it uses SC-FDMA, it is 2 to 3 dB less severe.[6] To first order, maximizing output power is the key objective to achieve LTE downlink PA linearity, so an optimum power match is used for the output stage.

Modulation bandwidth also imposes requirements on matching and bias circuitry. The modulation bandwidth is up to 20 MHz. The key concern is baseband products at 20 MHz. The HBTs have very high gain at these low frequencies. Matching circuits and bias circuits need to incorporate filtering to minimize these low frequency products. Otherwise, the low frequency products will limit power amplifier linearity. The high gain of the HBTs at low frequencies can also cause instabilities. Care must be taken in designing low frequency filtering in the matching and bias circuits to avoid possible oscillations and spurious outputs.

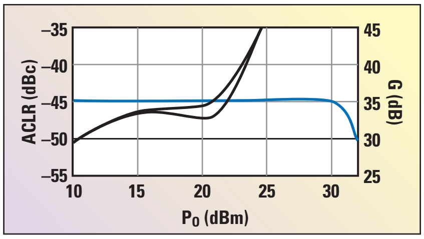

▲ *Fig. 3 Output performance of a typical LTE downlink power amplifier; ACLR (black traces) starts to increase significantly ~10 dB before gain (blue trace) compresses.*

SUMMARY

We have provided some background on LTE, specifically the downlink, and what it means to the PA designer. The LTE downlink signal has a high modulation bandwidth with many orthogonal carriers. This results in very high PAPR, and drives the entire PA design. We have gone through many of the choices a PA designer must make in addressing LTE downlink requirements and provided a roadmap to complete a successful design. This illustrates how the next generation of LTE PA for access points is being developed. There are more complex design approaches that have been taken for the uplink, where DC power is critically limited.[7] These too may find their way into access points in the future. ■

References

1. "Cisco Visual Networking Index: Global Mobile Data Traffic Forecast Update, 2010-2015," *Cisco White Paper*, June 1, 2011.
2. "Report: Netflix is Largest Source of Internet Traffic in North America," *PC Magazine*, May 17, 2011.
3. "Measuring ACLR Performance in LTE Transmitters," *Agilent Technologies Application Note*, January 7, 2010.
4. "LTE, Evolved Universal Terrestrial Radio Access, User Equipment Radio Transmission and Reception," Technical Specification - ETSI TS 136 101 v9.1.0.
5. B. Kim, J. Moon and I. Kim, "Efficiently Amplified," *Microwave Magazine*, August 2010, pp. 87-100.
6. L. de Temino, G. Bernrdinelli, S. Frattasi, K. Pajukoski and P. Morgensen, "Single-User MIMO for LTE-A Uplink: Performance Evaluation of OFDMA vs. SC-FDMA," *2009 Radio and Wireless Symposium Digest*, pp. 304-307.
7. "RFMD PowerSmart Platforms Achieve 4G Performance Milestone," *Microwave Journal*, January 2011.

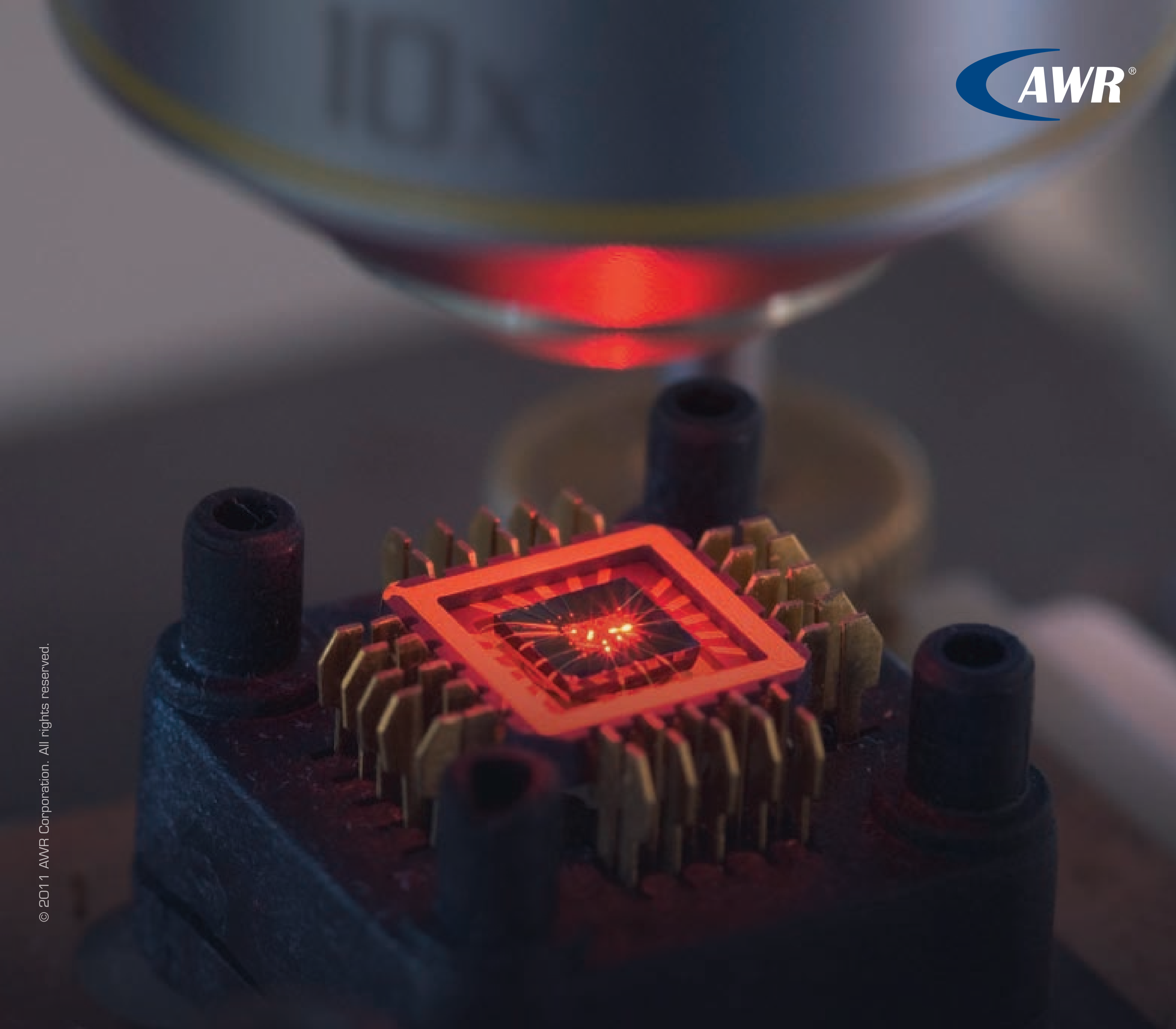

AWR®

Add a macroscope to your Microwave Office.™

See the big picture quickly in one design environment with VSS. Zoom in to make circuit tweaks. Then zoom out to see the system impact. VSS does system budget analysis and identifies sources of IM products, harmonics, and noise directly on your Microwave Office circuits. VSS's powerful simulator defines complex systems — radio and circuit designs, baseband signal processing, algorithmic development, and digital fixed-point implementations too. Grab a test copy at awrcorp.com/VSS.

Stop waiting and start designing™

VSS SYSTEM SIMULATOR

The Future of RFIC Test Strategy

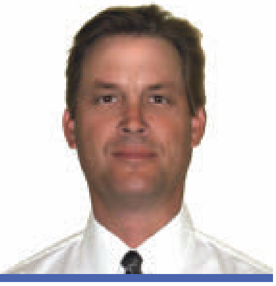

Ron Williamson *Aeroflex Test Solutions, Plainview, NY*

The future of Radio Frequency Integrated Circuit (RFIC) test strategy is a provocative topic these days. This is especially true for the consumer RF and connectivity integrated circuit (IC) markets, where ramping volumes and surging competition are shifting the market's mindset. Driven by cell phones, tablets, and other mobility devices, most RF devices are approaching commodity status, including the discrete power amplifier, front-end module, Bluetooth, WiFi and tuner segments. Price pressure is so extreme that a once-manageable test strategy is now overkill for low-end to mid-range devices. IC vendors are pulling all the punches to procure "just enough" production test capability.

For the past 20 years, standard automated test equipment (ATE) served this segment well. Competent RF technology led the way, augmented by reliable production worthiness. The general-purpose nature of production test was also suitable for the few silicon vendors whose product portfolio spanned the entire RF offering. But as we have seen in recent years, the technology has branched out. Multiple protocol standards, varying foundry processes and distinct Served Available Markets have created a more specialized supplier base.

This specialization has unearthed fertile soil for many new fabless companies. For example, in the Asia Pacific (APAC) region, accessible IC design technology and a maturing regional supply chain has fostered aspirations of dominating local markets. These players are especially sensitive to cost and are keen to "blaze a new trail" by adopting new test strategies. If these strategies are proven out, they will offer time-to-market advantages. These advantages may allow APAC suppliers to challenge the "blue chip" suppliers in the US and Europe in the years to come. However, the APAC suppliers have one primary dilemma – RF test is still an enigma in most Asian technology centers. Their local subcontracted manufacturers, although owners of many indigenous or legacy testers, possess limited RF test options. They see RF test capability as their final puzzle piece. They need to find a solution, either through low cost means and/or augmenting their current installed base with RF functionality.

These APAC "upstarts" are not the only IC vendors seeking alternative RF test solutions. IC manufacturers whose core competencies are digital or mixed signal are now integrating antennas into their devices. This creates significant test challenges. The IC manufacturing supply chain also possesses a large installed base of production test equipment with limited RF functionality. They want to view the RF pin as "just another device pin." But the question remains: How do they validate RF quality without overhauling their production strategy and/or excessively increasing their cost of test?

As we have seen in digital test over the past 20 years, the \$8,000/digital pin in 1993 has become less than \$500/pin in many current testers. Can the same economies be realized in RF? Commercial off-the-shelf (COTS) RF instrumentation is capable, proven, relatively inexpensive, and readily plays within industry standard form factors. Using these tools, can someone develop a cost-sensitive, focused solution for commoditized RF semiconductors? The ideal solution would:

- Meet the RF functionality requirements with seamless integration
- Be modular in nature, and offer a multitude of capability options
- Be production worthy with high reliability and throughput

- Stand alone, or assume a slave role for integration into a current tester environment

At Aeroflex, we believe the answer is yes – a solution can be developed. A precedent has already been set in semiconductor validation and characterization labs. These labs have successfully employed standard instruments to validate and debug their initial devices. VME, VXI and stand-alone instruments have all found a place in semiconductor test lore. However, the integration was usually custom, slow, cable-awkward and manual by nature.

Today's COTS instrumentation is a different beast. The PXI form factor has revolutionized the lab environment and is universally accepted. In the RF space, powerful instruments like 13 GHz sources and analyzers, vector network analyzers, single slot bi-directional port modules, local oscillators, intermediate frequency arbitrary waveform generators (AWG) and digitizers are one click away. Other non-proprietary standard technologies are building momentum as well. AXIe, PXI's big brother, has a quickly growing instrument portfolio, including RF AWGs, 48-channel digital pin electronics, 12-channel device power supplies, relay and load board controls, plus logic and protocol analyzers.

But the tipping point in RFIC ATE goes well beyond instrument functionality. Integration of the components by a team that understands semiconductor test is paramount. Moreover, PXI/AXIe instrumentation and infrastructure are proving to have exceptional reliability, fast data/signal busses and valuable multi-stage triggering. All of these benefits translate to key elements of a production test environment – high MTBF, fast test times and system coherency. The proof manifests itself in the cell phone manufacturing lines where 30 to 40 percent of all phones are tested with PXI solutions. Leveraging our cell phone success, coupled with the ever-increasing adoption of the PXI and AXIe form factors, Aeroflex recently introduced two industry standard, instrument-based test solutions that uniquely meet the four requirements above, including the AXRF RF Subsystem and AX-Series RF Characterization and Production Test System (PXI and AXIe).

In summary, competition and market dynamics in the consumer RFIC space has changed the industry mindset about RF product testing. Specialization and end-user product diversity opened doors for new and current IC vendors willing and eager to take risks for a market advantage. They see production test as a means to an end. They have pushed the test and measurement industry to accommodate their needs. This solution would not have come to fruition two years ago. Functionality alone did not create the tipping point. It took many intangibles to breach the precipice – customer adoption of PXI/AXIe instruments, proof of production worthiness in real world manufacturing, architectural improvements for fast test times with high accuracy, and most importantly, semiconductor-savvy teams to integrate the entire solution into a sophisticated, competent and user-friendly tool. ■

Coexistence of Terrestrial Microwave Point-to-Point Links and Wind Turbines

As one of the potential sources of alternative energy, wind turbines are considered an emerging industry and have been erected in many locations in the US, as well as around the world. Wind turbines work on the principle of conversion of the kinetic energy from wind into mechanical energy, which is then used to generate electricity. Wind turbines in large numbers are called wind farms and could potentially impact radio communications systems, including broadcasting stations, weather radars, airport radars and terrestrial microwave point-to-point systems.

Any time engineers are designing a new microwave link in a desolate area, they should investigate existence and proximity of wind turbines. This brief article will discuss and summarize some of the concerns engineers have to address during the microwave network design, in order to ensure a peaceful coexistence of microwave links and wind turbines. The same conclusions are also applicable to projects that might be considering a construction of a new wind farm in an area with existing microwave links.

WIND TURBINES AND WIND FARMS

1.5 MW turbines can be very large structures, with blades exceeding 67 m (220 feet) in diameter and tower heights exceeding 55 m (180 feet).[1] The wind farm concerns include the fact that they are composed of highly reflective materials, they can be up to 400 feet tall and have a large radar cross section (RCS), with blade tips spinning up to 200 mph; wind farms could have hundreds of these high profile structures in a relatively small area.[2]

Simply speaking, RCS is the measure of a target's ability to reflect radar signals in the direction of the radar receiver (which may or may not be collocated with the radar transmitter). Although it is difficult to actually calculate the RCS of a wind turbine, some measurements show that its value could be close to the RCS of a jumbo-jet. It is easy to conclude that a large wind farm could cause false alarms (or holes in the coverage in case they are ignored by the radar) on the screens of nearby airport radars, so planes flying over the wind farm may or may not be detected.

Wind farms are usually located in elevated and exposed regions, where they can experience an unobstructed exposure to the wind. This type of exposure is also preferred in fixed telecommunication installations, like microwave sites. There has been very little research done on this topic, which is becoming increasingly interesting as more and more wind farms are being constructed. Generally speaking, microwave engineers should carefully consider

Harvey Lehpamer
HL Telecom Consulting, San Diego, CA

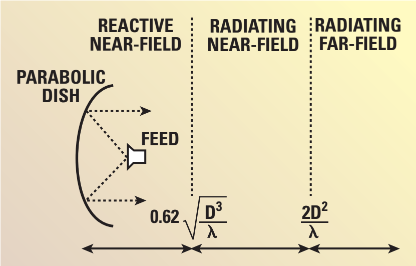

▲ *Fig. 1 Radiation fields of an antenna.*

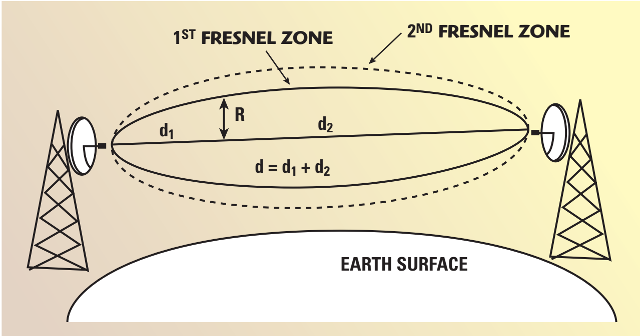

▲ *Fig. 2 Fresnel zones.*

three criteria that potentially could cause degradation of an RF communications system, such as near-field, diffraction and reflection/scattering.

NEAR- AND FAR-FIELD

The terms far-field and near-field describe the fields around an antenna or, more generally, around any electromagnetic radiation source. The names imply that two regions, with a boundary between them, exist around an antenna. Actually, as many as three regions and two boundaries exist, and it is important to notice that these boundaries are not fixed in space (see ***Figure 1***).

Usually, two- and three-region models are used. In the near-field, the field strength does not necessarily decrease steadily with distance away from the antenna, but it may exhibit an oscillatory character and, therefore, it is difficult to predict the antenna gain and radiation pattern in that region.[3]

Engineers perform microwave link engineering, including Fresnel's clearances and path profiles, based on the assumption that microwave antennas are in the far-field region, that is the distance between them is sufficiently large. Any large object (reflective or not), including wind turbines, in the near-field of the antenna may distort the radiation pattern of the antenna and, therefore, should be avoided.

CONCEPT OF THE FRESNEL ZONE

The concept of the Fresnel zone is an integral part of the terrestrial microwave point-to-point link design. The most common use of Fresnel zone information on a profile plot is to check for obstructions that penetrate the zone and calculate a possible diffraction. Fresnel zones are specified employing an ordinal number that corresponds to the number of half-wavelength multiples that represents the difference in radio wave propagation path from the direct path. The first Fresnel zone is, therefore, an ellipsoid whose surface corresponds to one half-wavelength path difference and represents the smallest volume of all the other Fresnel zones (see ***Figure 2***).

In microwave engineering, the radius of the first Fresnel zone is the parameter currently employed to establish appropriate clearance of the link from different types of obstacles. The general formula (assuming that $R_n \ll d_1$ and $R_n \ll d_2$) to calculate the radius of n^{th} Fresnel zone is approximated by:

$$R_n = \sqrt{\frac{n\lambda d_1 d_2}{d_1 + d_2}} \qquad (1)$$

In this formula, λ is a wavelength, R is a radius of the Fresnel zone, and d_1 and d_2 are distances from the antennas to the point of interest, and d is a microwave link length.

A more practical formula to calculate the radius of the first Fresnel zone in feet, which uses distances in miles, frequency in gigahertz, is given by:

$$R_{feet} = 72.1\sqrt{\frac{d_1 d_2}{f\left(d_1 + d_2\right)}} \qquad (2)$$

Diffraction theory indicates that the direct path between the transmitter and the receiver needs a clearance of at least 60 percent of the radius of the first Fresnel zone to achieve free-space propagation conditions.

If the geometry of the path is such

that an even-numbered Fresnel zone happens to be tangential to a good reflecting surface (such as a lake, highway, or smooth desert area, or wind turbines in this case), signal cancellation will occur as a result of interference between the direct and indirect (reflected) signal paths.

What is not included in this discussion is that the refractive properties of the atmosphere are not constant and the variations of the index of refraction in the atmosphere (expressed by the Earth-radius factor k) may force terrain irregularities to totally or partially intercept the Fresnel zone. A much more detailed discussion of the effects of climate on clearance requirements is given in reference 3.

MICROWAVE LINK ENGINEERING IN THE PROXIMITY OF WIND TURBINES

Perhaps the most dangerous situation is if the wind turbine is blocking or impinging the first Fresnel zone. Diffraction (obstruction) or reflection of radio waves by a wind turbine can degrade the performance of a point-to-point microwave link due to the effect of large blades rotating at approximately 32 rpm (typically there are two or three blades). Thus any significant interfering signal, such as a delayed multipath component, will fluctuate in signal level approximately 1.0 to 1.5 Hz.[4]

Based on some measurements, a single turbine can cause fades of 2 to 3 dB on microwave links with frequencies up to 18 GHz. A wind farm with only 17 turbines can produce up to 20 dB of fading if it is inside the Fresnel zone. Considering that the microwave link fade margin is typically 30 to 35 dB, this is a very significant loss of signal.[5]

It is important to remember that the horizontal axis of blade rotation varies in azimuth according to the wind direction, so this is not a static obstacle, like a tree or a building. Although typically 60 percent clearance of the first Fresnel zone is sufficient to guarantee undisturbed performance of the microwave link, in this situation the recommendation is to keep the first Fresnel zone completely, 100 percent clear. In addition, even a clear first Fresnel zone may not be sufficient, so a more stringent requirement of also keeping the second Fresnel zone clear should be implemented.

Signal reflection from the physical structure of a turbine propagating into the microwave receiver can potentially result in receiver's threshold degradation, resulting in a critical increase in the carrier-to-interference (C/I) ratio, usually expressed in decibels, depending on the modulation and coding schemes) requirement for the link. Care should be taken with respect to a possible multiple reflections from the individual turbines of a wind farm. A long string of wind turbines running in parallel with the microwave link could be especially detrimental.

CONCLUSION

The process of designing a microwave link in the vicinity of wind turbines follows the usual good practices of microwave engineering – avoid obstacles in the near-field of the antennas, keep first (and second, in this case) Fresnel zone clear of obstacles, and pay special attention to reflections when running microwave link in parallel to the long string of wind turbines. In some special cases, space diversity or some other method of reducing effects of multipath and improving reliability of the microwave link may be required. ■

References

1. M. Ragheb, "*Radar Signatures of Wind Turbines*," 2009.
2. S. Baron, "*Wind Turbines in the National Airspace System*," FAA, Presented to BLM Renewable Energy Summit, 2009.
3. H. Lehpamer, "*Microwave Transmission Networks – Planning, Design, and Deployment*," 2nd Edition, McGraw-Hill, New York, NY, 2010.
4. D.F. Bacon, "*Fixed-Link Wind-Turbine Exclusion Zone Method*," 2002 www.ofcom.org.uk.
5. B.S. Randhawa and R. Rudd, "*RF Measurement Assessment of Potential Wind Farm Interference to Fixed Links and Scanning Telemetry Devices*," ERA Technology Ltd., Surrey, UK, 2008, www.ofcom.org.uk.

Harvey Lehpamer, *PhD, is a licensed Professional Engineer in the Province of Ontario, Canada. He is an owner and the Principal Engineer of the HL Telecom Consulting, company in San Diego, CA. Lehpamer is an author of a number of technical articles and books: "Transmission Systems Design Handbook for Wireless Networks," Artech House, 2002, and "Microwave Transmission Networks - Planning, Design and Deployment," McGraw-Hill, 2004, and a Second Edition in 2010. The third book, "RFID Design Principles," was published by Artech House in 2008.*

Addressing Traffic and Channel Power Distributions in 3G Networks

Providing capacity to keep pace with the explosive growth in wireless data services is a highly complex task due to the time variant and geographically inhomogeneous nature of offered traffic. To ensure a consistent, high quality user experience, both site and carrier density must be tailored to match the offered traffic density, with sufficient margin to accommodate large fluctuations in traffic loading.

A white paper from ISCO International discusses the statistical distributions of traffic and interference from a network perspective, and how poor correlation between measured traffic and uplink channel power can be used to assess interference severity. Interference is a pervasive problem, and as networks strain to handle growth in wireless data traffic, the importance of identifying and resolving performance degradation due to interference is growing more acute.

Traditional approaches address severely impaired sites on a case-by-case basis, and are often identified by customer complaints of poor service quality. Applying a more network-centric approach, by jointly analyzing RTWP and traffic loading distributions to identify potential trouble sites, represents a more proactive approach to interference management that allows operators to identify RF impairments before they turn into customer complaints.

Figure 1 illustrates the distribution of traffic, ranked vs. site percentile from highest to lowest in five percent bins, for a typical urban 3G wireless network. If site coverage perfectly matched the geographical distribution of offered traffic, each bin would carry the same fraction of the total network traffic and the histogram would appear uniform. The actual distribution, however, is highly skewed: Sites in the first bin (the busiest five percent of sites) carry 19 percent of the total network traffic, and the busiest 25 percent carry half of the total traffic.

Read the complete white paper online at www.mwjournal.com/ISCOtraffic.

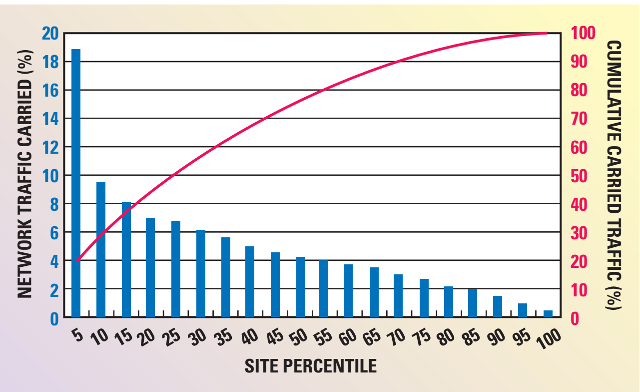

▲ *Fig. 1 Total percentage of network traffic carried vs. site percentile.*

Sean Cordone
ISCO International, Elk Grove Village, IL

AMPS
WiFi
TX
DCS
WLL
MMDS
VHF
UHF
CDMA
GSM
Wireless
Microcell
&
Reactel, Incorporated
Mobile
EGSM
UMTS
RX
WLAN
C1
C2
COM
Cellular
SMR
Crossband Coupler
PCS
REACTEL
AWS
8031 Cessna Avenue • Gaithersburg, Maryland 20879 • Phone: (301) 519-3660 • Fax: (301) 519-2447
For general inquiries, please email reactel@reactel.com • E-mail catalog@reactel.com to receive your Reactel Product Catalog or go online to www.reactel.com to download your copy today.
FM
Approvals
RoHS
3G

LTE-Advanced Physical Layer Design and Test Challenges: Carrier Aggregation

Achieving the ITU's IMT-Advanced 4G target peak data rates of 1 Gbps in the downlink and 500 Mbps in the uplink requires bandwidths that are wider than the maximum 20 MHz bandwidth specified in 3GPP Release 8/9 LTE. To achieve those targets, 3GPP Release 10 LTE-Advanced supports carrier aggregation, allowing two or more component carriers (CC) to be aggregated to create wider transmission bandwidths of up to 100 MHz. Most operators are unlikely to find 100 MHz of contiguous bandwidth in the available spectrum resources, so the ITU has allowed the use of both contiguous and non-contiguous carrier aggregation. In the latter case, the component carriers can be non-contiguous in the same spectrum band (intra-band) or non-contiguous in different spectrum bands (inter-band). This article presents an overview of carrier aggregation along with some of the associated design and test challenges from the physical layer perspective for both the base station and the user equipment (UE). The type of test equipment that will be required to tackle these challenges is also considered.

To meet different spectrum and deployment plans, 3GPP Release 8/9 LTE introduced six carrier bandwidths of 1.4, 3, 5, 10, 15 and 20 MHz. However, to achieve the ITU's IMT-Advanced 4G target downlink peak data rate of 1 Gbps, even wider bandwidths are required. IMT-Advanced sets the upper limit at 100 MHz, with 40 MHz the expectation for minimum performance. Because most spectrums today are occupied and 100 MHz of contiguous spectrum is not available to most operators, the ITU has allowed the creation of wider bandwidths through the aggregation of multiple component carriers. Carrier aggregation has been adopted in 3GPP Release 10, better known as LTE-Advanced.

Three aggregation scenarios are defined in Release 10: single-band (or intra-band) contiguous carrier aggregation, single-band non-contiguous carrier aggregation and multi-band (inter-band) non-contiguous carrier aggregation. Component carriers of the same or different bandwidths (1.4 to 20 MHz) may be aggregated.

Release 10 component carriers are essentially the same as the carrier bandwidths defined in Release 8/9. In this way, LTE-Advanced maintains backward-compatibility with LTE. A Release 10 UE, with carrier-aggregation reception or transmission capability, can simultaneously receive or transmit on multiple component carriers corresponding to multiple serving cells. However, a Release 8/9 UE can receive or transmit on a single component carrier corresponding to one serving cell only.

Martha Zemede
Agilent Technologies, Santa Clara, CA

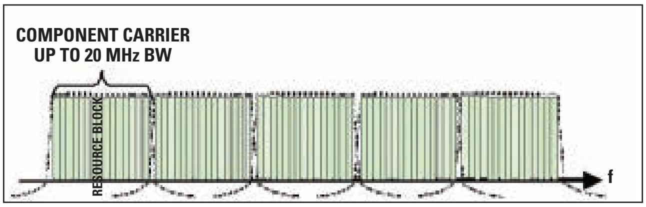

Fig. 1 Contiguous allocation of component carriers.

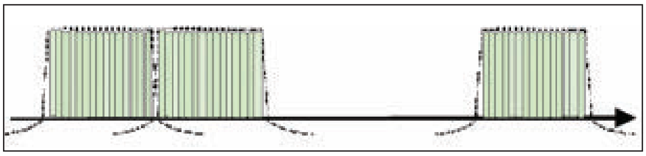

Fig. 2 Intra- or single-band non-contiguous allocation of component carriers.

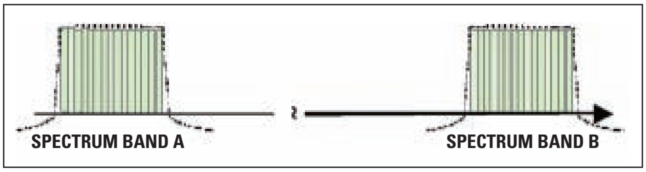

Fig. 3 Inter- or multi-band non-contiguous allocation of component carriers.

Figure 1 shows an example of inter-band carrier aggregation, in which five adjacent component carriers, each 20 MHz wide, covering the maximum 100 MHz LTE-Advanced bandwidth. For most operators today, this scenario is not realistic, since most operators do not have more than 20 MHz in a given frequency band. However, such contiguous allocation of component carriers may be realistic when new spectrum bands, such as 3.5 GHz, become available to operators in some countries.

Figure 2 shows an example of intra-band non-contiguous aggregation, in which the component carriers are separated within a single frequency band. This scenario can be applied if multiple operators share a network or if the frequency band allocated to an operator is fragmented.

Figure 3 shows an example of inter-band non-contiguous aggregation, in which component carriers belonging to different frequency bands (such as 1.8 and 2.6 GHz bands in some parts of Europe) are aggregated. Carriers aggregated in each frequency band can be contiguous or non-contiguous. The inter-band scenario for the downlink (base station to UE) is more realistic today because spectrum allocation for operators is often scattered across multiple frequency bands. However, for the uplink (UE to base station), this scenario would be very challenging because it would require multiple transceivers in the UE.

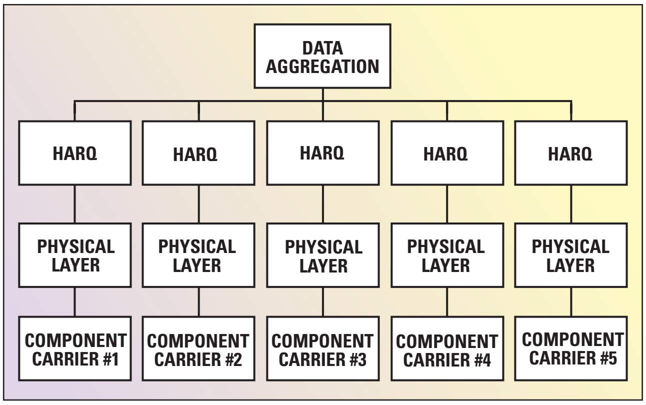

Fig. 4 Data aggregation from the PHY up to the MAC interface.

Mapping of the component carriers, from the physical layer (PHY) up to the medium access control (MAC) layer interface, is shown in ***Figure 4***. There is one transport block (in the absence of spatial multiplexing) and one Hybrid Automatic Repeat Query (HARQ) entity for each scheduled component carrier (HARQ is the control mechanism for retransmission). Each transport block is mapped to a single component carrier only. A UE may be scheduled over multiple component carriers simultaneously. The details of how the control signaling will be handled across the multiple component carriers are still being developed by 3GPP.

OPERATING BANDS FOR CARRIER AGGREGATION

The operating bands currently specified in Release 10 for LTE-Advanced carrier aggregation are defined in ***Tables 1*** and ***2***. These bands are defined for intra-band

TABLE I

INTRA-BAND CA OPERATING BANDS [3GPP TS 36.101 V 10.3.0 (2011-06)]

E-UTRA CA-Band	E-UTRA Band	Uplink (UL) Operating Band			Downlink (DL) Operating Band			Duplex Mode
		BS Receive/UE Transmit			BS Transmit/UE Receive			
		FUL_low-FUL_high			FDL_low-FDL_high			
CA_1	1	1920 MHz	to	1980 MHz	2110 MHz	to	2170 MHz	FDD
CA_40	40	2300 MHz	to	2400 MHz	2300 MHz	to	2400 MHz	TDD

TABLE II

INTER-BAND CA OPERATING BANDS [3GPP TS 36.101 V 10.3.0 (2011-06)]

E-UTRA CA-Band	E-UTRA Band	Uplink (UL) Operating Band			Downlink (DL) Operating Band			Duplex Mode
		BS Receive/UE Transmit			BS Transmit/UE Receive			
		FUL_low-FUL_high			FDL_low-FDL_high			
CA_1-5	1	1920 MHz	to	1980 MHz	2110 MHz	to	2170 MHz	FDD
	5	824 MHz	to	849 MHz	869 MHz	to	894 MHz	

contiguous and inter-band non-contiguous cases. As more deployment scenarios are agreed upon based on operator input, more band definitions will be added to the specification independent of the Release version.

DESIGN CHALLENGES

Carrier aggregation brings new technical challenges, especially for the LTE-Advanced UE. The complexity of the UE's radio frequency (RF) front-end implementation can vary greatly, depending on which type(s) of carrier aggregation are supported, with contiguous carrier aggregation being the least complex. In Release 10 devices, contiguous carrier aggregation will not exceed two component carriers or 40 MHz maximum. It may be possible to support this configuration with a single wideband transceiver in the UE.

For non-contiguous component carrier allocations, the UE will have to use multiple transceivers or a single, very wide wideband transceiver. Using multiple transceivers may be realistic in the sense that such configuration requires only the addition of parallel paths to process each spectrum band, as in current multi-band devices. However, using multiple transceivers also increases the size and cost of the mobile device and shortens the battery life.

In the case of the wideband transceiver, a single transceiver must process the multi-band non-contiguous aggregation using wideband RF components. There are two main issues with this approach. First, as the bandwidth increases, the effective noise increases as well. Second, with a wider bandwidth, more undesired signals are likely to be received from other services. Thus for non-contiguous aggregation, most proposals today are trending toward the use of multiple transceivers instead of a single wideband approach.

In addition to increasing the RF front-end complexity, using simultaneous non-contiguous transmitters creates a highly challenging radio environment in terms of spur management and self-blocking. Because these challenges particularly impact UE design, more work needs to be done before inter-band carrier aggregation can be successfully introduced in the uplink. This is expected in 3GPP Release 11. However, for the LTE-Advanced base station, intra- and inter-band cases are defined in Release 10.

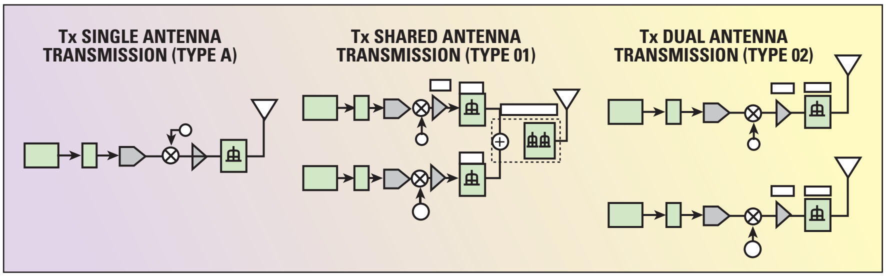

▲ *Fig. 5 Release 10 transmission architecture options [3GPP TR36.807 VO.1.0 (2010-08)].*

DEFINING THE TEST REQUIREMENTS

Some of the test complexity in designing and testing LTE-Advanced equipment arises from the existence of simultaneous transceiver chains that require simultaneous tests of multiple transmitters. ***Figure 5*** shows three different transmission architectures defined in Release 10. Type A supports two scenarios: intra-band contiguous carrier aggregation with a maximum of two Release 8 component carriers and a maximum uplink bandwidth of 40 MHz; and inter-band non-contiguous carrier aggregation with a maximum of two Release 8 component carriers. In this case, simultaneous transmission on both bands is not supported. Intra-band non-contiguous is not supported.

Type D1 currently supports two scenarios. One is intra-band contiguous carrier aggregation with a maximum of two Release 8/9 component carriers and a maximum uplink bandwidth of 40 MHz. The other is inter-band non-contiguous carrier aggregation with a maximum of two Release 8 component carriers, a maximum uplink bandwidth of 20 MHz, and support of simultaneous transmission on both bands. Type D1 has the capability to support intra-band non-contiguous carrier aggregation in future releases of the specification.

Type D2 currently supports two scenarios. One is intra-band contiguous carrier aggregation with a maximum of two Release 8/9 component carriers, a maximum uplink bandwidth of 40 MHz, and uplink MIMO support to address uplink peak data rate requirements. The other is inter-band non-contiguous carrier aggregation with a maximum of two Release 8 component carriers, a maximum uplink bandwidth of 20 MHz, and support of simultaneous transmission on both bands. Type D2 also has the capability to support intra-band non-contiguous carrier aggregation in future releases of the specification.

The different transmission configurations introduce a number of test challenges. For example, if a transmission configuration uses multiple transmitter antenna connectors, most of the evolved Node B (eNB) RF performance requirements will need to be applied at each antenna connector. Current LTE specifications for the eNB will be reused for LTE-Advanced as much as possible. For example, Release 8/9 requirements for transmitted signal quality tests (frequency error, EVM and downlink reference signal power) will be applied for each component carrier in a carrier aggregation scenario. The requirement for time alignment error between component carriers is being considered and the operating band unwanted emissions requirements for carrier aggregation transmissions have been aligned with those defined for the Release 8 multiple-carrier base station.

However, translating test requirements from Release 8/9 to Release 10 presents a number of difficulties. In the case of inter-band aggregation, synchronization must be maintained between the multiple transceivers, to allow simultaneous error vector magnitude (EVM) measurements on multiple component carriers. It has therefore been proposed for uplink to specify EVM only for those cases in which the power density is the same for both carrier allocations.

With intra-band non-contiguous carrier aggregation, there is a gap between the component carriers in which other technologies (for example, GSM or W-CDMA) could be transmitted. Physical layer transmit

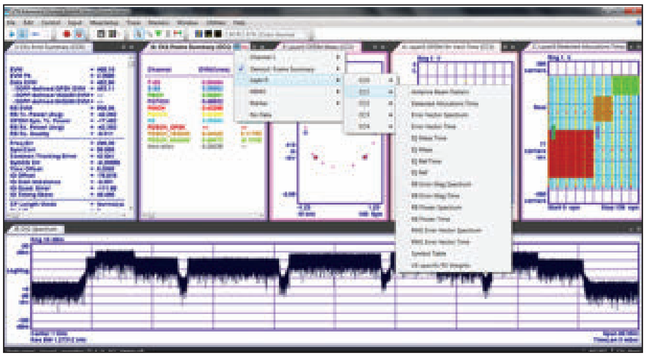

▲ *Fig. 6 Agilent 89600 VSA Software for LTE-Advance controls two signal analyzers and measures up to five components simultaneously displaying results of each in a separate trace.*

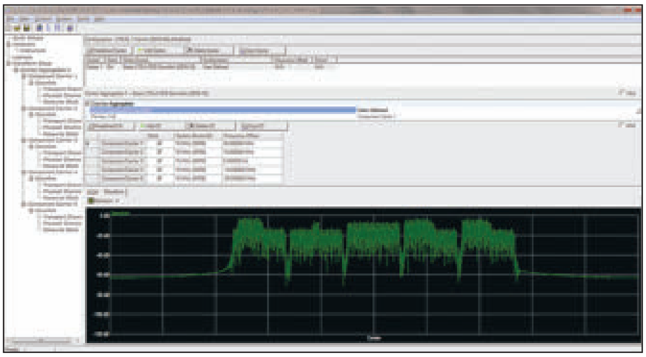

▲ *Fig. 7 Agilent Signal Studio Software generates an aggregated signal consisting of five contiguous component carriers.*

and receive measurements will need to be extended across the gap, to assess the interference caused by the co-existing, uncoordinated systems. This scenario increases the difficulty of defining limits to out-of-band emission tests, such as adjacent channel power and spectrum emission mask, and the details are still being worked out.

Multicarrier in-band emissions for the uplink pose another problem. The Release 8/9 requirement, based on a single wanted contiguous physical resource block (PRB), is too complex to scale up to a generalized multi-carrier requirement. Alternative ways of specifying carrier aggregation in-band emissions are being studied. The intention is to specify a general requirement that would apply, regardless of whether a single or dual transmitter architecture is used.

Characterizing the LTE-Advanced UE or eNB power amplifier presents still another RF challenge. The different carrier aggregation configurations will stress the amplifier in different ways, because each will have different peak-to-average ratios. In the case of the UE, a single transceiver may be used for contiguous carrier aggregation. Although the design is similar to that of a Release 8/9 UE, the power amplifier in the LTE-Advanced UE has to be capable of covering the wider bandwidth created by carrier aggregation.

TEST TOOLS FOR LTE-ADVANCED CARRIER AGGREGATION

Testing carrier aggregated signals requires instruments that can generate and analyze multiple-component carriers simultaneously. The key word here is "simultaneously." One of the biggest challenges facing engineers working on LTE-Advanced is how to analyze the multiple-component carriers at the same time, especially in the case of inter-band carrier aggregation, as no signal analyzer on the market has a bandwidth wide enough to cover multiple frequency bands. Existing LTE measurement instruments are capable of analyzing component carrier in one frequency band at a time, but to capture and analyze multiple component carriers, in different frequency bands simultaneously, requires advanced tools.

This problem has been solved by using two signal analyzers, each tuned to a relevant frequency band and synchronized. The analyzers are controlled with software developed specifically for LTE-Advanced testing that has the ability to acquire all the component carriers simultaneously from the two synchronized instruments, demodulate the captured signals and analyze them all simultaneously. An example of the results is shown in ***Figure 6***. The software displays each component carrier measurement in a separate trace.

LTE-Advanced downlink and uplink signals compliant to the Release 10 standard are required to test power and modulation characteristics of components and transmitters. In ***Figure 7***, signal generation software is used to create an aggregated signal with five component carriers. The software's built-in tools, such as CCDF, can be used to analyze compression and evaluate the required amplifier power back-off for different signal configurations.

CONCLUSION

Although the concept of carrier aggregation is simple, the changes it introduces at the physical layer are complex. With the introduction of carrier aggregation, asymmetric uplink and downlink allocations will become commonplace, driven by different numbers of component carriers in the uplink and downlink signals, the different bandwidths of component carriers that can be aggregated and the resulting combinations of component carrier number and bandwidth in an aggregated signal. The number of test cases for carrier aggregation would quickly become unmanageable if all contiguous and non-contiguous intra-band and inter-band combinations were considered. How to limit the allowed allocations in order to minimize the number of test scenarios is a major topic of discussion within the 3GPP. ■

Martha Zemede *graduated from San Jose State University in 2000 with a bachelor's degree in electrical engineering and has taken postgraduate studies in wireless communications at Stanford University. She is working in the Microwave and Communications Division of Agilent Technologies, as an applications expert for 3GPP LTE/LTE-Advanced Signal Analysis solutions. In the past 11 years with Agilent, Zemede has worked in supporting the cellular communication technologies in Agilent's signal analyzers, as well as product marketing positions. She has also developed and led training courses and workshops on cellular wireless technologies for thousands of customers worldwide.*

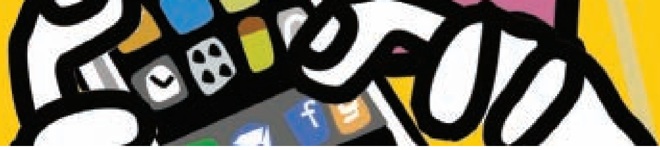

MICROWAVE JOURNAL REVIEWED EDITORIAL BOARD

THE MASTERS OF MIMO

A Compact MIMO Antenna using ZOR Split Ring Resonator Radiators with a Decoupling Structure

This article presents a novel compact MIMO antenna for mobile communication devices, which has miniaturized antennas with increased isolation and operates in the WiMAX and LTE high bands. Each of the proposed element antennas is designed to have the in-phase electric field distributions of the zeroth order resonance (ZOR) in the form of a CRLH type split ring resonator (SRR), which is much smaller than the conventional SRRs and other antennas for MIMO communications. These antennas can be placed in close vicinity, using a small planar mushroom decoupling structure between them, in order to meet the required isolation level. The design is carried out by full-wave electromagnetic simulations, which prove the ZOR characteristic of the antennas and the suppressed interference from one antenna to the other. This proposed MIMO antenna was fabricated and measured to show a return loss better than 10 dB, an isolation greater than 12 dB and a radiation efficiency over 50 percent in the WiMAX and LTE high bands for both antennas. The total size is 26 × 5.5 × 2 mm, which fits within half of the top-edge of the ground of handset phones.

As people are taking advantage of the convenience of mobile and wireless communications, the demands are increasing on technological evolution in the field of telecommunications. From communication methodologies to portable device fabrication, developers are facing challenges and striving to tackle the problems. In the meantime, smartphones have provided numerous application programs and mobile Internet services, started through WiMAX and LTE technologies. The handset phones for the aforementioned function should be robust, in a complicated and tough environment, to guarantee the quality of communication and be small for commercial success. This is heavily determined by the hardware of the phones, including the antennas.

The multi-input multi-output (MIMO) antenna was proposed to handle the harsh wireless communication environment, by providing

SEONGRYONG YOO AND
SUNGTEK KAHNG
University of Incheon, Incheon, Korea
JONG-GUK KIM
LG Innotek Co. Ltd., Ansan, Korea

diversity in RF signal transmission and reception and has motivated the antenna community, where size reduction is a hot issue, along with high isolation between multi antennas. A. Mak et al.[1] introduced a set of antennas with a structure that traps the near-field coming from one antenna to the other, based upon a local current loop disconnecting a fictitious enlarged loop of current in order to secure the isolation. The antennas have acceptable radiation pattern and isolation, but in terms of size, the radiators and the trap take the top edge and two sides of the handset ground. K. Payandehjoo et al.[2] adopted an EBG geometry to increase the diversity gain by preventing coupling between two antennas. However, the size exceeds the industrial standard and the working frequency is away from the WiMAX band. X. Wang et al.[3] described two microstrip-fed antennas. Their vertical and layered radiating parts stand perpendicular to the handset stratified ground by folding and periodically meandering a decoupling structure for improving the isolation. Although it has an isolation greater than 12 dB, this structure is a microstrip-fed, monopole-type, decoupling geometry, with three dimensionally folded radiators, the volume of which takes most of the ground.

It is pointed out that these antennas and the decoupling structure should be size-reduced while having antenna performances meeting the industrial requirements. Recently, metamaterials (MTM) technologies were introduced and have suggested alternative ways to overcome the limitations in improving electrical performances and reducing the sizes of components and resonators.[4,5] Lumped elements of series capacitance and shunt inductance are loaded in a transmission line to generate nonlinear dispersion characteristics due to the composite right- and left-handedness (CRLH), including the ZOR due to the in-phase field over a corresponding MTM resonator. While the CRLH and ZOR are mentioned with the electromagnetic bandgap (EBG) of an array of the mushroom (a patch connected to the ground through a pin),[4] the SRRs are adopted to fit a resonator into a confined area, on account of the end-gap and inter-ring capacitances.[6] The SRRs create a resonance, so they can be applied to not only to filters, but also to antennas.[7] The SRR is designed to make one antenna, but its size is approximately 30 × 40 mm and not appropriate for the mobile MIMO antenna, considering that two antennas of its kind and the decoupling structure between them, will result in an overall horizontal length over 90 mm. This shortcoming results from the fact that their SRRs do not have the ZOR or metamaterial properties.

In this article, a miniaturized MIMO antenna that has novel antenna elements and a decoupling geometry is described. It aims to satisfy size, antenna performance and isolation required by WiMAX and LTE high band communications. The antenna elements look similar to SRRs, but they are much smaller than ordinary SRR antennas, since the proposed structure has a CRLH configuration and a ZOR field distribution. To suppress the coupling between the novel antennas, a planar mushroom is placed between them. Because this mushroom is planar, it is conveniently and inexpensively formed in the bottom grounding surface of the substrate of the MIMO antenna geometry. The design goes through full-wave simulations for monitoring and tuning S_{11}, radiation pattern, ZOR field and isolation of the proposed antenna. It is then fabricated on an FR4 substrate and experimentally tested on the board of a real mobile phone. As a result, it is revealed that the return loss, isolation and radiation efficiency are better than 10 dB, over 12 dB, and over 50 percent, respectively, in the WiMAX and LTE high bands, for both the antennas, whose overall size is 26 × 5.5 × 2 mm. This is less than half of the top-edge of the handset ground, even when the proposed MIMO antenna is mounted in a mobile phone platform.

TABLE I
MIMO ANTENNA DESIGN SPECIFICATIONS

Item	*Specification*
f_0, Bandwidth	2.4 GHz, ≥ 100 MHz
Application	WiMAX, LTE high band
Return loss (S_{11})	≤ 10 dB
Radiation efficiency	≥ 50%
Isolation (S_{21})	≥ 12 dB
Overall antenna length	< 30 mm
Condition for test	Coaxial feeding, On the real board

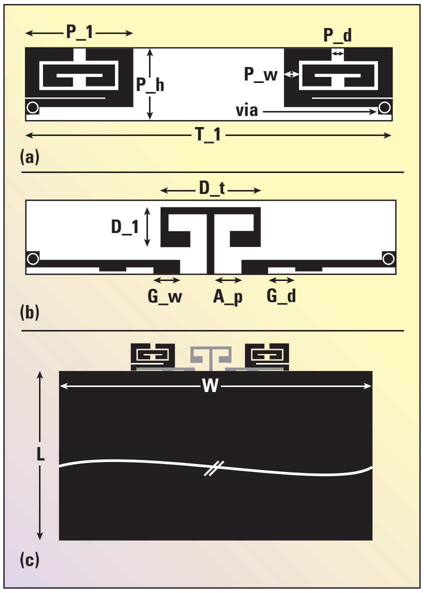

▲ *Fig. 1 Structure of the proposed MIMO antenna (a) top surface, (b) bottom surface and (c) antenna at top edge of handset ground.*

DESIGN OF THE PROPOSED MIMO ANTENNA

Prior to the design, the specifications shown in ***Table 1*** are addressed. The element antennas have similarity to SRRs in that the inner open-gap ring is surrounded by the outer ring. Different from the ordinary SRRs, one corner of the outer ring is connected to a transmission line (upper transmission line or UTL), that is coupled through the electric field and current to another transmission line (lower transmission line or LTL), attached to the ground. The element antennas' SRRs and the UTL are placed on the top surface of the 2 mm-thick FR4 substrate, whose bottom surface has the feeding points with the handset ground, the planar mushroom and the LTL as shown in ***Figure 1***. The handset ground has an area (W × L) of 50 × 80 mm. The aim of the proposed design is to reduce the size of the resultant antenna to less than 70 percent of W. Since the conventional SRR has a right-handed resonance, at first sight, it seems improper for effective size-reduction. So each of the anten-

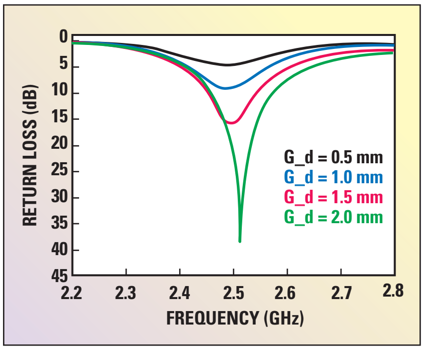

▲ *Fig. 2 Return loss of the proposed antennas as a function of G_d.*

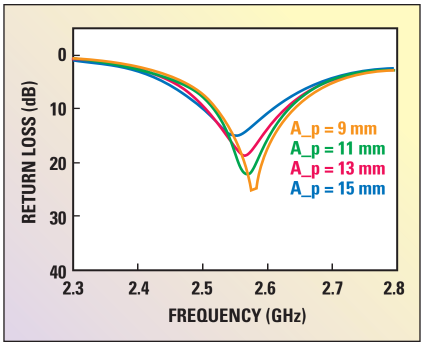

▲ *Fig. 3 Return loss of the proposed antennas as a function of A_p.*

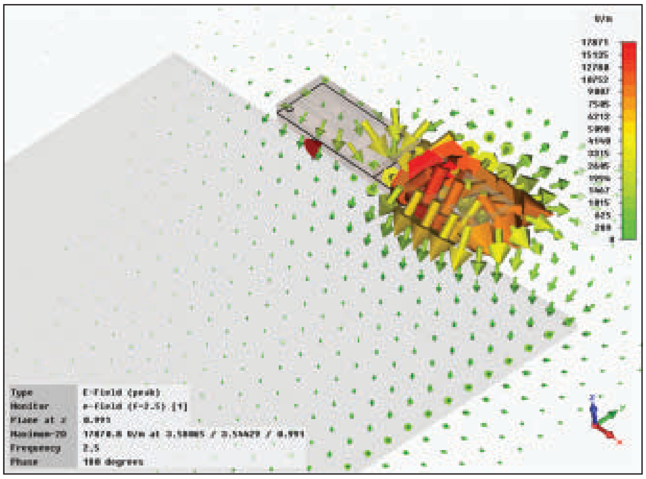

▲ *Fig. 4 In-phase electric field distribution of the ZOR at the center frequency.*

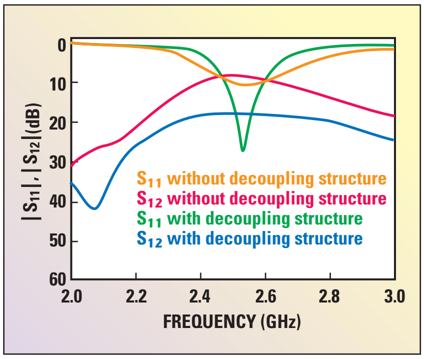

▲ *Fig. 5 Return loss and isolation before and after placing the planar mushroom.*

nas, 1 and 2, has the SRR play the role of the series capacitance (C_L) and part of the series inductance (L_R) in implementing the CRLH characteristics. Simultaneously, the electric field coupling and current flowing between the upper and bottom transmission lines are equivalent to part of the shunt capacitance (C_R) and the shunt inductance (L_L), respectively. Besides, the bottom transmission line provides inductance and capacitance factors of the right-handed transmission line as L_R and C_R. In principle, the approach of the CRLH equivalent circuit is very similar to that of Jang et al.[5] The factors are adjusted to have the CRLH ZOR, which enables the proposed SRR to be much smaller than the conventional SRRs. The ZOR field will be given later in the article. Pursuing the realization of the metamaterial ZOR properties for this structure, the following parametric studies are conducted. Along with G_w, G_d accounts for the impedance matching and manipulating the main part of CR. In ***Figure 2***, the return loss (S_{11}) is plotted for different values of G_d, with P_l, P_h, P_d, P_w and G_w set to 10, 5, 1, 0.8 and 2.0 mm, respectively. G_d ranges from 0.5 to 2.0 mm and four samples are taken. With a 10 dB criterion, G_d values of 1.5 mm and above are acceptable. This implies that the proposed miniaturization method requires a certain collective shunt capacitance of CR, maintaining G_d. ***Figure 3*** shows the return loss of the antenna as a function of the feeding positions (A_p), with respect to the decoupling structure, with the other parameters P_l, P_h, P_d, P_w, G_w and G_d fixed as 10, 5, 1, 0.8, 2.0 and 2.0 mm, respectively. A_p is varied from 9 to 15 mm. It shows that once A_p is set over 9 mm with the other parameters chosen as above, the change of the return loss seems insensitive to the distance between the planar mushroom and either of the element antennas. In a similar manner, all the physical dimensions are found to achieve the antenna functions required by the WiMAX and LTE high bands, through impedance matching and electromagnetic interactions between the radiators, transmission lines, feeding points, handset ground, etc. Before moving to the proposed planar mushroom to decouple the interference between antennas 1 and 2, the ZOR characteristic is proven by the electric field distribution over either of the element antennas. This full-wave simulation is performed with the CST-MWS.[8] While the conventional SRRs have an out-of-phase electric field distribution, in a physical structure that is manipulated for the same resonance frequency and larger than the proposed antenna, the ZOR antenna with a size 0.2 times that of the top-edge is resonant at the center frequency. The ZOR results in the in-phase electric field vectors (all directed upward) and contribute the lower interference to the neighboring antenna (see ***Figure 4***).

Next, a planar mushroom is proposed to enhance the isolation. As far as the MIMO antenna is dealt with, the isolation between the multiple antennas is one of the most crucial factors in the design. The less the antennas are correlated or coupled, the higher the antenna isolation is, which means the signal survives multiple reflection and fading in a wireless environment with higher probability. As shown in ***Figure 5***, with the help of the planar mushroom as the decoupling structure, the isolation is increased from 8 to 19 dB, which is far better than the specification. When the MIMO antenna is designed for increasing the best isolation, the return loss (S_{11}) is optimized as 27 dB. These values, S_{11} and S_{12}, are preparation for the possible degradation that can be caused by the physical placement on the real phone platform. Besides, the frequency response of the two antennas with the decoupling structure of D_t of 6.5 mm and D_l of 3.0 mm, the surface current densities are plotted in ***Figure 6*** to determine how the increased isolation is obtained. Obviously, the planar mushroom, centered in the entire MIMO antenna system, decouples the connection between antennas 1 and 2. In other words, the decoupling structure draws the surface current due to the near-field from one excited antenna and

BROADBAND

GaN POWER AMPLIFIERS

with frequency ranges in excess of 10 octaves 3 to 10 W

FEATURES:

- Single bias, 30V
- Excellent gain flatness over very wide bandwidths
- Withstands high baseplate temperatures or surges in RF or DC power without compromising reliability
- Various models available that operate from 30 MHz to 4 GHz
- Built-in over/reverse voltage protection
- Temperature and over-current protection

MODEL NUMBER	FREQUENCY RANGE (GHz)	GAIN (dB, Min.)	GAIN FLATNESS (±dB, Max.)	NOISE FIGURE (dB, Max.)	VSWR IN/OUT	P1dB (dBm, Min.)	Psat (dBm, Min.)	NOMINAL PEAK CURRENT @ 30V (mA)
AMFG-3F-00030100-60-33P	0.03-1	42	1.5	6	2:2	34	36	750*
AMFG-3F-00030300-60-33P	0.03-3	40	2	6	2:2.2	33	35.5	750*
AMFG-3F-00030400-60-32P	0.03-4	40	2	6	2:2	32	35	750*
AMFG-3F-00040250-60-33P	0.04-2.5	40	2	6	2:2.2	33	35.5	670
AMFG-3F-00050100-50-34P	0.5-1	40	1.5	5	1.8:1.8	34	37	750*
AMFG-3F-00230025-30-37P	0.23-0.25	50	1	3	1.5:2	37	40	250*
AMFG-3F-00500350-60-32P	0.5-0.35	40	1.75	6	2:2.2	33	35	600*
AMFG-3F-00700380-60-35P	0.7-3.8	40	2	6	2.5:2.5	35	39	1500
AMFG-3F-00800220-60-35P	0.8-2.2	40	1.5	6	2:2	35	38	900*
AMFG-2F-01000300-60-35P	1-3	40	2	6	2:2.2	35	39	1500
AMFG-2F-01000200-60-38P	1-2	35	2	6	2:2	36	37	1500

Notes: Psat is defined as the output power where a minimum of 3 dB gain compression takes place.
Higher power available, please contact MITEQ.
* 12V version available.

For additional information, please contact our Sales Department at (631) 439-9220 or e-mail components@miteq.com

MITEQ

100 Davids Drive • Hauppauge, NY 11788
TEL.: (631) 436-7400 • FAX: (631) 436-7430
www.miteq.com

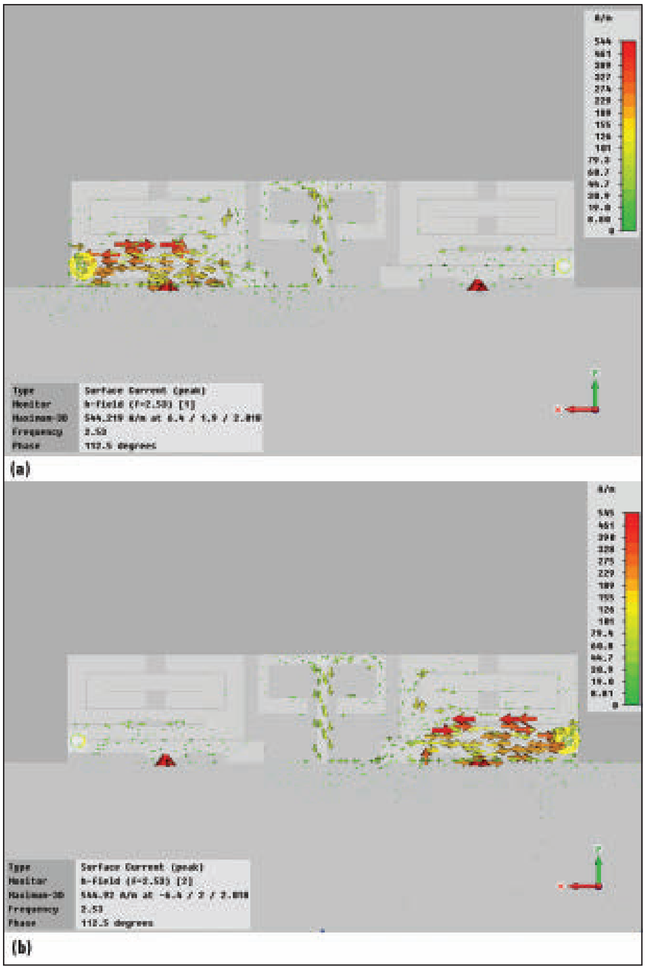

▲ *Fig. 6 Surface currents on isolated antennas (a) from antenna 1 to antenna 2 and (b) from antenna 2 to antenna 1.*

▲ *Fig. 7 Proposed antenna tested on a real board.*

plays the role of a trap. Consequently, the isolation between the element antennas is enhanced.

FABRICATION AND MEASUREMENT

After the design phase, based upon the theoretical and numerical approaches, the proposed antenna was manufactured for experimental verification. As simulated in a full-wave analysis frame, a simple microstrip MIMO antenna is made on an FR4 substrate with $\varepsilon_r = 4.3$ and a thickness of 2 mm. The overall size of the proposed antenna is 26 × 5.5 × 2 mm, which amounts to just within half of the top-edge of the ground of handset phones. ***Figure 7*** shows the antenna mounted on the phone platform with a cover. After extra trimming work, the proposed antenna was simulated to give the return loss and isolation as shown in ***Figure 8***. The best performance ($|S_{11}|$ and $|S_{22}| < -25$ dB, $|S_{21}| < -19$ dB) is achieved, in case of degradation in manufacturing and real environment test. The measured return loss and isolation ($|S_{11}|$ and $|S_{22}| < -22.5$ dB, $|S_{21}| < -12$ dB) complies with the specifications. ***Figure 9*** presents the radiation patterns in the E- and H-planes, where the two antennas have similar omni-directional far-field plots, desirable in MIMO communications, even with the isolation of over 12 dB. Lastly, the radiation efficiency and peak and average gains are measured as shown in ***Figure 10***. The plot shows that the efficiency is over 50 percent. Simultaneously, the peak gain is 2.25 dBi at the center frequency, which is acceptable to the industry, with an average gain of –2.7 dB. In summary, all the electrical performances and the physical size of the proposed MIMO antenna are compliant to the design specifications.

CONCLUSION

This article has presented a novel compact MIMO antenna, which has enhanced isolation between very small antenna elements. The antennas are miniaturized for the first time with the proposed ZOR SRRs, which have the in-phase field behavior and a size

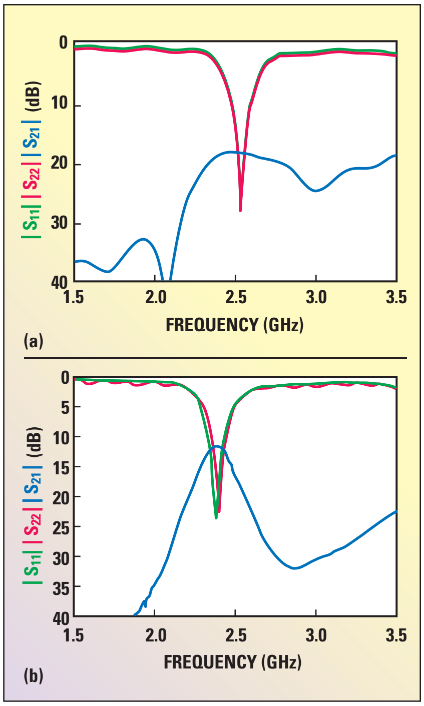

▲ *Fig. 8 Antenna performance while mounted on a real board (a) simulation and (b) measurements.*

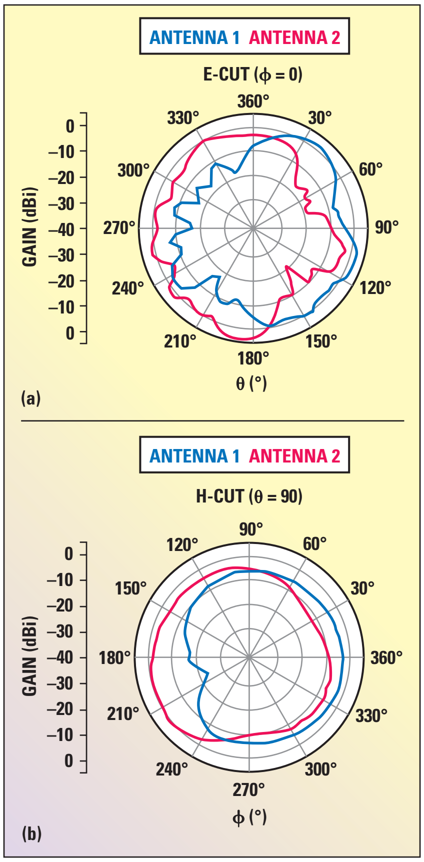

▲ *Fig. 9 Radiation patterns of the antenna (a) E-plane and (b) H-plane.*

of 0.2 times the top-edge of the handset ground. A planar mushroom, used

(Continued on page 42)


You Have Our Undivided
ATTENTION
EWT
www.ewtfilters.com
We understand how critical your applications are. That's why you'll always have our *Undivided Attention*.
Offering more than 40 years of experience in custom design & manufacturing of RF and Microwave filters and filter based products to 50 GHz.
Military • Commercial
Wireless • Space
Eastern Wireless TeleComm, Inc.
Tel: 410.749.3800 Fax: 410.749.4852
sales@ewtfilters.com

LTE PAs Offer Fast, Powerful Wireless Data Options

Consumers are demanding more from their mobile devices, including increased bandwidth. They have become accustomed to the near universal data connectivity of smartphones and tablets, including applications that continually demand higher and higher data rates. Given the variety of LTE frequency bands, and the range of preferred power levels, RFMD has developed a family of LTE-compatible power amplifiers for data connectivity applications. They are summarized in ***Table 1***.

TABLE I

RFMDs FAMILY OF POWER AMPLIFIERS FOR LTE DATA CONNECTIVITY

Part Number	Frequency Range (GHz)	Integration	Linear Power (dBm)	Supply Voltage (V)	Current (mA)
RF5602	2.3 to 2.7	Unmatched PA	21 to 23	3.3 to 5	350 to 450
RF5603	3.3 to 3.8	Unmatched PA	23	3.3	425
RF5607	1.9 to 2.7	Unmatched PA	22	5	350
RF5612	2.5 to 2.7	Matched PA	22	3.3	470
RF5623	3.3 to 3.8	Unmatched PA	24	5	600
RF5652	2.3 to 2.7	Unmatched PA	28	5	1200
RFFM7600	2.3 to 2.7	Matched PA+SPDT	24	5	650

As can be seen, a wide range of LTE bands can be covered by these PAs. The RF5607, for example, has a large frequency coverage capability of 1.9 to 2.7 GHz. This allows the customer to tune to a desired frequency band within this range. The RF5602 is similar and offers higher output power with less frequency coverage. It can also be efficiently operated at lower power with a reduced V_{cc}. The linear power listed for each of these amplifiers is for a nominal linearity requirement, and varies depending on the specific modulation used. The RF5612 is intended for uplink applications, the others are primarily intended for the downlink. Many of the amplifiers in Table 1 can also be used in WiMAX applications, typically at higher output powers. RFMD continues to add to its LTE power amplifier family, with higher power levels in particular, soon to be available.

RF5607

The RF5607 is a versatile member of RFMD's LTE power amplifier family. It is

RF Micro Devices
Greensboro, NC

POWER AMPLIFIER SOLUTIONS

[*Broad Selection - COTS and Custom Products*]

COMMUNICATIONS

MODULES	SKU	Start (MHz)	Stop (MHz)	Pout (Watt)	Size (Inch)	Gain (dB)
	1058	1	100	300	8.3x6.4x1.2	18
	1067	0.01	500	25	7.0x5.0x1.3	44
	1094	20	520	100	6.4x3.4x1.1	50
	1100	20	1000	80	6.4x3.4x1.1	49
	1119	500	2500	50	7.4x3.6x1.1	46
	1164	800	3000	50	6.4x3.4x1.1	50

Wireless Infrastructure MODULES	SKU	Start (MHz)	Stop (MHz)	Pout (Watt)	Size (Inch)	Gain (dB)
	7086	869	894	16	4.4x6.7x1.1	49
	7083	1930	1990	30	5.1x6.7x1.2	49
	7082	1930	1995	16	4.4x6.7x1.1	49
	7084	2110	2170	16	4.0x5.5x1.3	49

SYSTEMS	SKU	Start (MHz)	Stop (MHz)	Pout (Watt)	Size	Gain (dB)
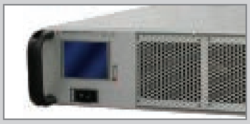	2073	1	100	1000	R5U	60
	2101	20	500	500	R5U	56
	2126	20	500	1000	R5U+R5U	60
	2066	500	1000	1000	R5U+R5U	60
	2151	500	2500	200	R3U	52
	2154	20	3000	250	C19U	54
	2153	700	3800	200	R3U	54

- *Amplifier products from 10 KHz to 6 GHz*
- *LDMOS and GaN technologies - optimized size, weight, efficiency*
- *Selection of COTS models available from inventory at Richardson RFPD*
- *Multi-function HPA solutions built per customer specification*

Empower RF Systems has extensive experience with Multi-Function, Highly-Integrated Assemblies. Customer-specific requirements are met by incorporating Integrated Filters, T/R switches, DC/DC Converters, Forward/ Reverse Power detectors and RCV LNAs into the Amplifier.

Certified to ISO 9001:2008
TÜVRheinland®
Precisely Right.

www.EmpowerRF.com

EMPOWER
RF SYSTEMS, INC.

316 West Florence Ave., Inglewood, CA 90301 USA, Phone: +1(310)412-8100, Fax: +1(310)412-9232

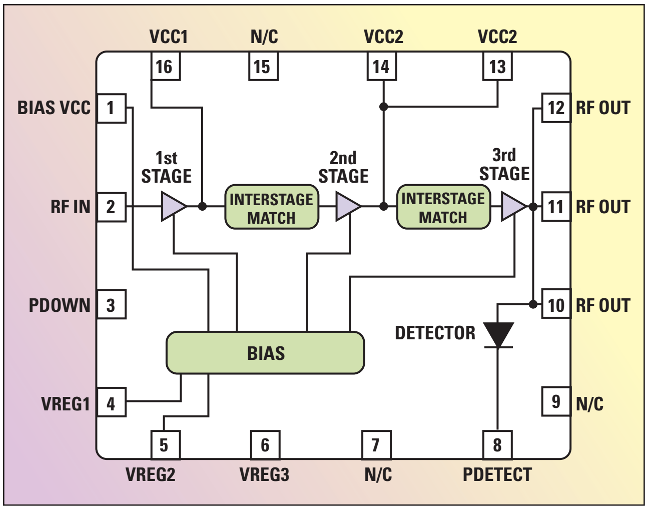

▲ *Fig. 1 Block diagram of the RF5607.*

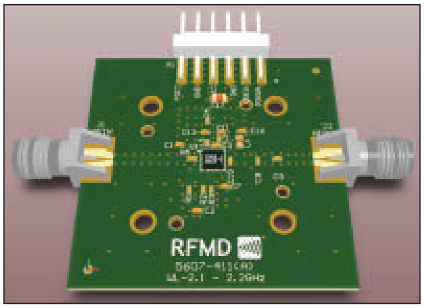

▲ *Fig. 2 The RF5607 LTE downlink PA application board for 2.1 to 2.2 GHz operation.*

designed using RFMD's InGaP HBT process. The block diagram, ***Figure 1***, shows that this is a three-stage power amplifier with integrated power detection and active bias control. All stages use a 3 × 20 μm dual emitter HBT unit cell. Two cells are used in the first stage. The second and third stages are scaled up to 8 and 32 cells, respectively.

The PA operates in Class AB mode. The second harmonic termination at the output is implemented with an on-chip capacitor and an in-package down bond. The first and second stages are each biased with a two-diode emitter follower. RFMD's proprietary active bias circuit supplies bias to the final stage while providing low impedance for linear operation over the operating range.

A unique feature of the RF5607 is that the input and output matching networks are off chip. Interstage matching is broadband to cover the entire 1.9 to 2.7 GHz frequency range. Actual applications are in much narrower bands within this range. Ultimate performance is critically dependent on output match and to a lesser extent on input match. Therefore, optimized matching for specific LTE downlink bands has been developed for implementation off-chip. ***Figure 2*** shows an application board for 2.1 to 2.2 GHz operation. The application boards for other bands are identical, only the values of the matching components change.

The schematic, with matching components optimized for a 2.1 to 2.2 GHz LTE downlink is shown in ***Figure 3***. The RF5607 uses a 3 × 3 mm QFN package. ESD protection is included on all pins to both Human Body Model (HBM) and Charged Device Model (CDM) requirements. The exact band of operation is tunable with external components.

The key performance attributes for an LTE power amplifier are power, ACLR and current consumption. Typical power and linearity for the RF5607 are shown in ***Figure 4***. As shown, ACLR remains well below the -44 dBc requirement up to 22 dBm output power. At that point, nonlinearities resulting from the large peak to average power ratio (PAPR) of the modulated signal begin to degrade ACLR. The RF5607 actually provides -45 dBc ACLR.

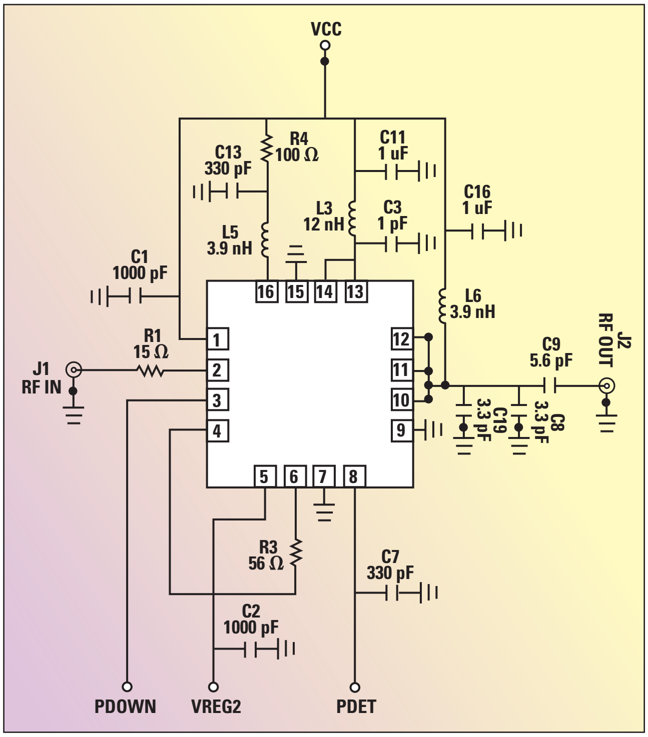

▲ *Fig. 3 Schematic of the RF5607 in a 2.1 to 2.2 GHz application.*

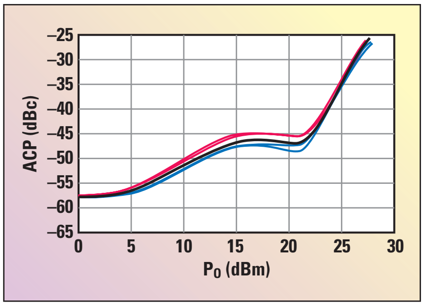

▲ *Fig. 4 Typical linearity performance of the RF5607 with a 10 MHz modulated LTE signal at frequencies between 2.11 and 2.17 GHz.*

Gain and current consumption are also important power amplifier characteristics. They are shown versus output power in ***Figure 5***. Note how gain is only lightly compressed even at the full LTE rated power of 22 dBm. This highlights the very linear operation that LTE downlinks demand. The current consumption is below 330 mA, even at 22 dBm. Current increases gradually from about 230 mA at quiescence. Since the output stage operates in deep Class AB, the low impedance active bias

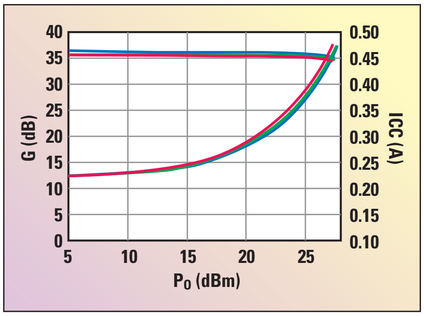

▲ *Fig. 5 Typical gain and current consumption performance of the RF5607 with a 10 MHz modulated LTE signal at frequencies between 2.11 and 2.17 GHz.*

(Continued on page 38)

GPS RFIC Preventing LightSquared and Other LTE Interference

Tahoe RF Semiconductor has introduced the industry's first single chip integrated dual-channel (L1 and L2 bands) GPS RFIC that provides 60 dB of dynamic range in high level interfering environments. The TRFS15011 was developed to address the use of position information in a wide variety of industrial and consumer electronic products where high level interferers may exist. Specifically, because of the impending FCC frequency allocation of the Mobile Satellite System (MSS) frequency band to terrestrial transmitters, commercial GPS receivers may need to operate in environments with high levels of interference. However, commercial GPS receivers currently do not have sufficient dynamic range to mitigate interfering signals from MSS transmitters. One possible solution is to use highly selective filters, but these filters are costly and bulky.

The TRFS15011 reaches new levels of functional integration for high dynamic range GPS receivers. It embodies high levels of integration and combines Tahoe RF Semiconductor's proprietary wireless signal integrity implementation to deliver superior interferer mitigation, lower system cost and eliminate the use of highly selective external filter solutions. The TRFS15011 is currently the only integrated solution that allows GPS receivers to operate in the presence of a high power interferer from terrestrial MSS band transmitters.

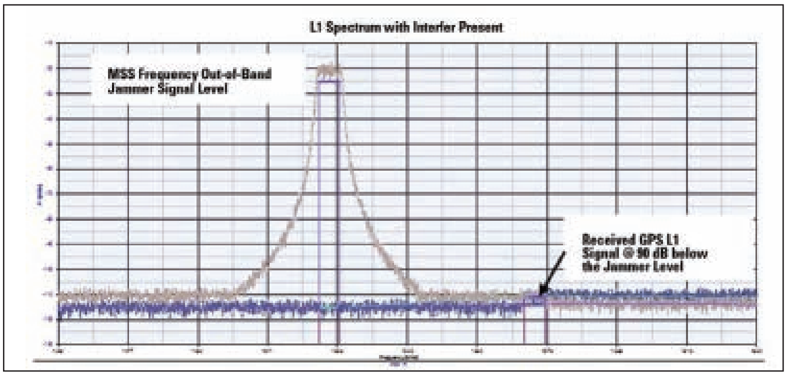

Fig. 1 Interferer and GPS signal.

DYNAMIC RANGE AND POTENTIAL INTERFERER FROM TERRESTRIAL MSS BAND TRANSMITTERS

The GPS L1 band is from 1560 to 1590 MHz. The proposed portion of the MSS band that will be used by terrestrial transmitters is 1526 to

TAHOE RF SEMICONDUCTOR
Auburn, CA

1536 MHz. The MSS anticipated power level at the transmitter is 32 dBW. With free space path loss, the input of a GPS receiver antenna could be as high as -20 dBm. The L1 signal level difference compared to the interferer can be as much as 90 dB (see ***Figure 1***).

New GPS receivers need to operate in the presence of high level interfering signals. Current GPS RF receivers typically do not operate over more than 18 dB of dynamic range. The embedded filtering in most GPS RF receivers is not sufficient to suppress the interferer and typically requires highly selective external filter solutions to mitigate interference as illustrated in Figure 1.

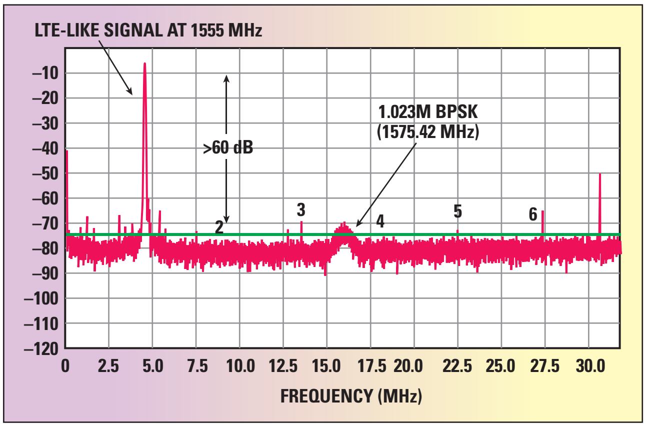

Fig. 2 FFT of the output with CW tone representing LTE interferer and GPS signal.

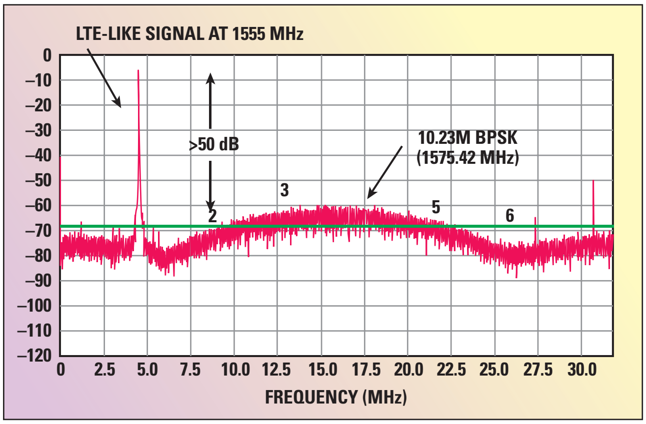

Fig. 3 FFT of the output with CW tone representing LTE interferer and GPS signal.

TRFS15011 PERFORMANCE

The TRFS15011 integrates high dynamic range 12-bit analog-to-digital converters (ADC) and full receive paths for both L1 and L2 bands. The result is a fully integrated L1/L2 GPS receiver with 60 dB instantaneous dynamic range, providing significant power savings over more discrete systems. Commercial GPS receivers are hampered by low resolution ADCs, which are used in an effort to conserve power. The TRFS15011 solves this problem by including two programmable ADC modes – a low power mode with 3 bits of resolution and a high dynamic range mode with 12 bits of resolution.

PERFORMANCE IN LTE ENVIRONMENTS

A single-tone interferer at 1555 MHz was inserted at the front-end of the TRFS15011 along with a low power GPS-like narrowband signal. The signals were down-converted and sampled with the high resolution ADC. The spectral plot of the output shown in ***Figure 2*** represents the typical dynamic range of the TRFS15011 that can be further improved, if needed, with external filtering and baseband processing.

Of more concern is how the receiver processes wider bandwidth signals. A single-tone interferer at 1555 MHz was inserted at the front-end of the receiver along with a low power GPS-like wideband signal. The signals were down-converted and sampled with the high resolution ADC. The spectral plot of the output is shown in ***Figure 3***. The TRFS GPS receiver has enough instantaneous dynamic range to mitigate a high level interferer signal such as the terrestrial MSS.

DEVICE DESCRIPTION

The GPS receiver block diagram is shown in ***Figure 4***. The dual fractional-N synthesizers are completely integrated. The received signal is level controlled by the internal AGC where each signal path includes an RF isolation amplifier, RF mixer, variable gain amplifiers and lowpass filter before the ADCs. There is a low resolution mode with reduced current and lower linearity for low power operation. With minimal external components, the TRFS15011 provides an integrated low cost solution for the interference that is inevitably to come from reallocation of FCC frequency use.

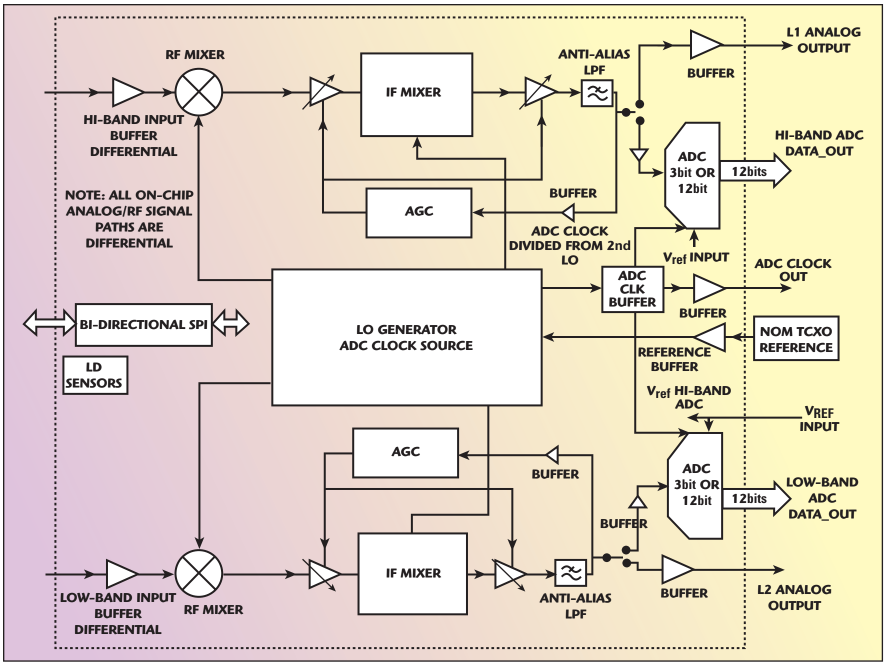

Fig. 4 Block diagram.

Tahoe RF Semiconductor,
Auburn, CA (530) 823-9786,
sales@tahoerf.com.
www.tahoerf.com.

Intermod Squad: Low PIM Cable Assemblies

Dubbed the Intermod Squad, San-tron has developed a new series of low PIM cable assemblies that feature intermodulation performance as low as -181 dBc with an eSeries 7/16 connector terminated on TFlex-402 cable. Typical performance across the lineup of assemblies terminated with eSMA and eSeries Type Ns is -162 dBc. The eSMA cable assemblies perform from DC to 20 GHz and the eSeries Type N cable assemblies perform from DC to 18 GHz. These assemblies are phase and attenuation stable, provide excellent shielding, support UL/NEC Plenum class CMP, are corrosion resistant, and are low in weight and highly flexible.

The key component in San-tron low PIM cable assemblies are their latest series of connectors. eSeries connectors, which include SMA (trademarked as eSMA), Type N, TNC and 7/16 styles, offer evolved cable/connector transitions. The repeatability of these transitions from the cable into the connector is key to the consistent high performance of these cable assemblies. The center contact is a solder-free connection so the transition is controlled to machined tolerances via an internal stop within the bodies, which are much tighter than the variations seen by cable assembly personnel and solder joints. Another advantage of the elimination of this center conductor solder joint is that it precludes the heat induced damage to the dielectric densities that would affect changes in the dielectric constant.

Reliability is improved with these connectors with an extended ferrule that is crimped onto the body that provides longitudinal protection out past the solder wick line, which is a traditional failure point. For added protection, dual wall heat shrink is positioned within the saddle of this crimp ferrule and further extends the strain relief from this wick line offering high reliability in applications that involve repeated flexure.

The Albaloy plating provides a robust surface that easily accepts the braid solder joint and supports corrosion resistance per salt fog testing. The eSMA center contacts are BeCu; they are plated gold over a copper strike providing excellent RF performance, corrosion resistance and control over porosity. The eSeries N and 7/16 center contacts are plated silver over a copper strike, which contains cost versus gold, and also provides good RF performance and corrosion resistance.

VENDORVIEW

**San-tron Inc.,
Ipswich, MA
(978) 356-1585,
www.santron.com.**

(Continued from page 34)

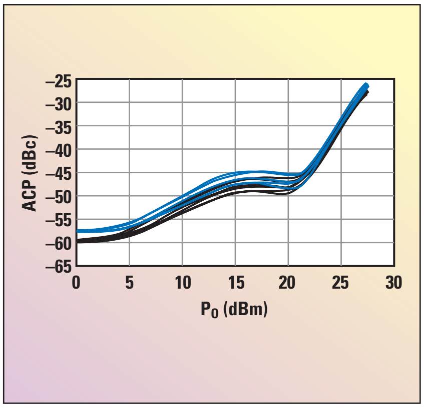

▲ *Fig. 6 Typical linearity performance of the RF5607 with a 10 MHz modulated LTE signal (blue) and a 5 MHz W-CDMA modulated signal (black) at frequencies between 2.11 and 2.17 GHz.*

network allows current to increase so that linearity is maintained as drive level grows.

Figure 6 shows the power and linearity performance of the RF5607 with both a LTE downlink signal and a W-CDMA signal. LTE has a wider modulated bandwidth and a higher data rate than W-CDMA. This increases the linearity demands on the system and on the PA. As Figure 6 shows, this can be directly seen in power amplifier performance. Linearity is 1.5 to 2.5 dB better with the W-CDMA signal.

LTE provides users with very high data rates in mobile devices enabling streaming multimedia and supporting the growth of social networking and the push to cloud computing. LTE imposes unique system requirements and presents challenges to the power amplifier designer, particularly of the downlink. RFMD has developed a family of products to address these needs. They cover the key downlink frequency bands, provide an ACLR of better than -44 dBc and provide efficient operation with LTE modulation bandwidths of up to 20 MHz.

**RF Micro Devices,
Greensboro, NC
(336) 664-1233,
www.rfmd.com.**

Company Showcase

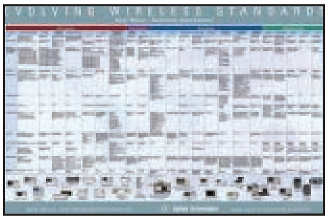

Wireless Standards Poster

VENDORVIEW

Gain greater insight into wireless design and test with the new Agilent Evolving Wireless Standards poster. Agilent offers one place to review the latest evolving wireless technologies any time. This FREE poster is designed to give information about wireless test for greater understanding of the wireless connectivity technologies with a full range of design and test solutions. Order your Agilent Wireless Standards poster at www.agilent.com/find/postermwj.

Agilent Technologies Inc.,
Santa Clara, CA (800) 829-4444, www.agilent.com.

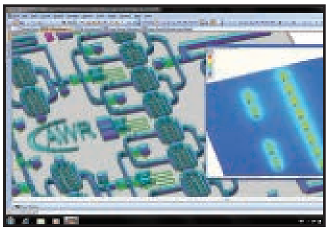

Product Portfolio

VENDORVIEW

AWR Corp. dramatically reduces development time and cost for products employed in wireless, high speed wired, broadband, aerospace and defense, and electro-optical applications. The 2011 version of its product portfolio – Microwave Office™, Visual System Simulator™, AXIEM® and Analog Office® – features electrical-thermal MMIC co-simulation design flow, simulation-state management technology, yield analysis/optimization via a graphical shape-based manipulation approach, envelope simulator and asynchronous electromagnetic (EM) simulation support.

AWR Corp.,
El Segundo, CA (310) 726-3000, www.awrcorp.com.

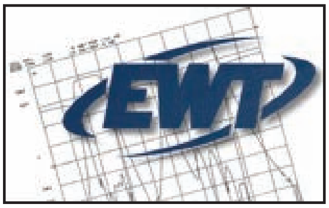

EWT: Where Performance Counts

VENDORVIEW

Eastern Wireless TeleComm Inc. (EWT) specializes in custom design and manufacture of RF and microwave filters and filter-based products for mobile communications applications. The staff encompasses more than 50 years of combined experience in the design, development, and high volume manufacturing of cavity and waveguide filters to 50 GHz and lumped element filters up to 10 GHz. All of the company's products are manufactured to strict guidelines set forth in its ISO:9001 compliant quality system, ensuring the highest level of product performance and reliability. Through utilization of the company's in-house machining capabilities and state-of-the-art manufacturing processes, rapid turn-around is standard. EWT can develop any cavity, lumped element, waveguide, or wireless filter to meet your needs. Visit EWT online to request a quote today.

Eastern Wireless TeleComm Inc.,
Salisbury, MD (410) 749-3800,
www.ewtfilters.com.

Compact Communications Amplifier Module

VENDORVIEW

The PCM3R3SCO (SKU 7091) is one of a series of communications amplifiers. This 900 MHz compact linear power amplifier is one of a series that covers 450, 700, 800, 900, 1800, 1900 and 2100 MHz bands and is suitable for use in commercial LTE networks and public safety wireless communication applications. The amplifier employs latest generation LDMOS device technology and is highly efficient. The amplifier has an advanced built-in predistortion engine with wide instantaneous correction bandwidth, which ensures low distortion and wide dynamic range operation. Efficiency of up to 40 percent is possible in this series where the high performance is achieved by employing advanced RF design techniques. Empower RF's ISO:9001 Quality Assurance Program assures consistent performance and the highest reliability.

Empower RF Systems Inc.,
Inglewood, CA (310) 412-8100,
www.empowerrf.com.

Low PIM Power Divider/ Combiners

VENDORVIEW

LOW PIM (-150 dBc typical) two-way through 16-way power divider/combiners are optimized for excellent performance across all wireless bands from 0.698 to 2.700 GHz and their rugged construction makes them ideal for both base station and in-building wireless systems. Weather-proof models are also available. Always available from STOCK to four weeks ARO in N, SMA, BNC or TNC connector configurations for your next generation equipment deployments. Made in the USA – 36 month warranty.

MECA Electronics Inc.,
Denville, NJ (866) 444-6322, www.e-meca.com.

Component CD Catalog

VENDORVIEW

MITEQ recently released its full-line CD Components Catalog (CD-02M), which offers one of the most comprehensive displays of standard and custom capabilities in the industry. The CD includes thousands of pages of product specifications, outline drawings, test data, manufacturing flow diagrams, and a wide assortment of technical application notes.

MITEQ,
Hauppauge, NY (631) 439-9220, www.miteq.com.

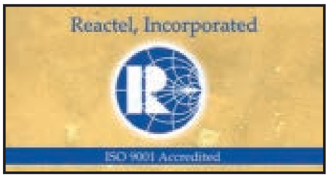

Filters, Multiplexers and Multifunction Assemblies

VENDORVIEW

Reactel offers a variety of filters, multiplexers and multifunction assemblies for the mobile communication industry. Reactel's experienced engineers can come up with a creative solution for all of your Tx, Rx or Co-site requirements. Reactel has designed a broad range of filters from high power units operating to 5 kW and beyond to extremely small ceramic units that are suitable for handheld or portable applications. The company's product line includes bandpass, lowpass, highpass and notch filters as well as multiplexers and multi-passband filters. Offering fast turnaround, competitive pricing and high quality, Reactel can satisfy most any requirement you may have.

Reactel Inc.,
Gaithersburg, MD (301) 519-3660,
www.reactel.com.

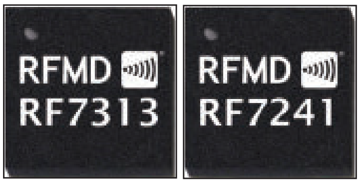

Power Amplifiers

The RF7241 and RF7313 represent an extensive family of high efficiency 3G/4G power amplifiers addressing the vast majority of the global frequency bands. Optimized for use with DC-DC converters, this family of 3G/4G PAs delivers industry-leading peak efficiency – directly translating into increased data usage time, increased battery life, and lower thermal dissipation. The 3G/4G handset OEMs can leverage these unique benefits to influence end user perceptions of handset quality, raising the value of the OEM's devices.

RFMD,
Greensboro, NC (336) 664-1223, www.rfmd.com.

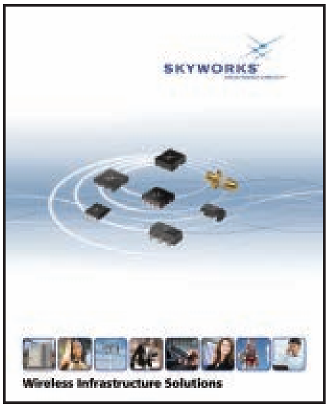

Wireless Infrastructure Solutions

VENDORVIEW

Skyworks' broad portfolio of RF/microwave products includes solutions for today's demanding wireless infrastructure systems, including cellular base stations, WiMAX access points, land-mobile radio systems and point-to-point radio links. Skyworks offers components and subsystems from the antenna connection to the baseband output, including low noise amplifiers, power amplifiers, general-purpose amplifiers, mixers, modulators, demodulators, phase shifters, switches, attenuators, detectors, directional couplers, hybrid couplers, power splitters/combiners, ceramic filters and resonators, plus discrete control components, including PIN, tuning varactor, Schottky diodes and chip attenuators.

Skyworks Solutions Inc.,
Woburn, MA (781) 376-3000, www.skyworksinc.com.

Mobile Communication Catalog

This new edition of SPINNER's mobile communication catalog has been extended and adapted to the needs on the wireless communications market. You can find SPINNER's new MultiFit™ connector family and the range of jumper cables with the innovative SPINNERFlex™ Hybrid Jumper. The "MNCS® – Mobile Network Combining System" – has been considerably extended – e.g. with several new multiplexers for all current systems from LTE700 to LTE2600. The "Analog Fiber Optic Links" for the supply of remote antennas and repeaters are totally new.

SPINNER GmbH,
Munich, Germany (Europe): +49 89 12601-0, USA: (770) 263-6326,
www.spinner.group.com.

(Continued from page 30)

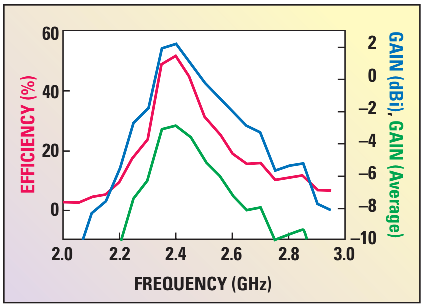

▲ *Fig. 10 Gain and efficiency of the antenna.*

as the decoupling structure between antennas 1 and 2, suppresses the mutual coupling and improves the isolation. Through full-wave simulations, the ZOR properties of the antennas and the decoupling between them have been proven. The antenna has been fabricated and tested in a real phone platform, showing a return loss better than 10 dB, an isolation greater than 12 dB and a radiation efficiency over 50 percent in WiMAX and LTE high bands, for both antennas, which have a total size of 26 × 5.5 × 2 mm. Considering these performances, this proposed antenna can be employed for developing small MIMO communication systems. ■

ACKNOWLEDGMENT

Sungtek Kahng, as the principal author with the University of Incheon, would like to thank LG Innotek for providing great opportunities to work on the MIMO antenna development. This work is part of a patent being filed.

References

1. A.K. Mak, C.R. Rowell and R.D. Murch, "Isolation Enhancement Between Two Closely Packed Antennas," *IEEE Transactions on Antennas and Propagation*, Vol. 56, No. 11, November 2008, pp. 3411-3419.
2. K. Payandehjoo and R. Abhari, "Employing EBG Structures in Multiantenna Systems for Improving Isolation and Diversity Gain," *IEEE Antennas and Wireless Propagation Letters*, Vol. 8, 2009, pp. 1162-1165.
3. X. Wang, Z. Feng and K.M. Luk, "Pattern and Polarization Diversity Antenna With High Isolation for Portable Wireless Devices," *IEEE Antennas and Wireless Propagation Letters*, Vol. 8, April 2009, pp. 209-211.
4. C. Caloz, C. and T. Itoh, "Electromagnetic Metamaterials: Transmission Line Theory and Microwave Application," John Wiley & Sons, Somerset, NJ, 2006.
5. G. Jang, S. Kahng, J. Ju, J. Anguera and J. Choi, "A Novel Metamaterial CRLH ZOR Microstrip Patch Antenna Capacitively Coupled to a Rectangular Ring," *2010 IEEE APS URSI Conference Digest*, pp. 1-4.
6. R. Marques et al. "Metamaterials with Negative Parameters: Theory, Design and Microwaves Applications," John Wiley & Sons, Somerset, NJ, 2008.
7. X. Yang, Z. Yu, Q. Shi and R. Tao, "Design of Novel Ultra-wideband Antenna with Individual SRR," *Electronics Letters*, Vol. 44, 2008, pp. 1109-1110.
8. www.cst.com, April 2011

Seongryong Yoo *received his bachelor's degree in engineering from the University of Incheon (UI), Incheon, Korea, in 2010. He is working on his master's degree on radio science and engineering at the Department of Information and Telecommunication Engineering in the University of Incheon. His research fields are antennas, microwave components and metamaterials.*

Sungtek Kahng *received his doctorate in electronics and communication engineering from Hanyang University, Korea, in 2000, with specialty in radio science and engineering. From 2000 to early 2004, he was with the Electronics and Telecommunication Research Institute, where he worked on numerical electromagnetic characterization and developed RF passive components for satellites. In March 2004, he joined the Department of Information and Telecommunication Engineering at the University of Incheon, where he has continued research on analysis and advanced design methods of microwave components and antennas, including metamaterial technologies, MIMO communications and wireless power transfer.*

Jong-Guk Kim *received his master's degree in mechatronics engineering from Gwang-ju Institute of Science & Technology (GIST) Graduate School, Gwang-ju, Korea, in 2004, with the design and analysis of X-Band mixer-type phase detectors. He is working on his doctorate in management of technology in the University of Sungkyunkwan, Suwon, Korea. In June 2004, he joined the department of Network Solution Group at the LG Innotek Co. Ltd.*

Sales Representatives

Carl Sheffres, Publisher

Ed Kiessling, Traffic Manager

Eastern and Central Time Zones
Chuck Boyd
Northeast Reg. Sales Mgr.
(New England, New York, Eastern Canada)
685 Canton Street
Norwood, MA 02062
Tel: (781) 769-9750
FAX: (781) 769-5037
cboyd@mwjournal.com

Michael Hallman
Eastern Reg. Sales Mgr.
(Mid-Atlantic, Southeast, Midwest)
4 Valley View Court
Middletown, MD 21769
Tel: (301) 371-8830
FAX: (301) 371-8832
mhallman@mwjournal.com

Pacific and Mountain Time Zones
Wynn Cook
Western Reg. Sales Mgr.
208 Colibri Court
San Jose, CA 95119
Tel: (408) 224-9060
FAX: (408) 224-6106
wcook@mwjournal.com

International Sales
Richard Vaughan
International Sales Manager
16 Sussex Street
London SW1V 4RW, England
Tel: +44 207 596 8742
FAX: +44 207 596 8749
rvaughan@horizonhouse.co.uk

Germany, Austria, and Switzerland (German-speaking)
WMS.Werbe- und Media Service
Brigitte Beranek
Gerhart-Hauptmann-Street 33,
D-72574 Bad Urach
Germany
Tel: +49 7125 407 31 18
FAX: +49 7125 407 31 08
bberanek@horizonhouse.com

Israel
Oreet Ben Yaacov
Oreet International Media
15 Kineret Street
51201 Bene-Berak, Israel
Tel: +972 3 570 6527
FAX: +972 3 570 6526
obenyaacov@horizonhouse.com

Korea
Young-Seoh Chinn
JES Media International
2nd Floor, ANA Bldg.
257-1, Myungil-Dong
Kangdong-Gu
Seoul, 134-070 Korea
Tel: +82 2 481-3411
FAX: +82 2 481-3414
yschinn@horizonhouse.com

Japan
Katsuhiro Ishii
Ace Media Service Inc.
12-6, 4-Chome,
Nishiiko, Adachi-Ku
Tokyo 121-0824, Japan
Tel: +81 3 5691 3335
FAX: +81 3 5691 3336
amskatsu@dream.com

China
Michael Tsui
ACT International
Tel: 86-755-25988571
Tel: 86-21-62511200
FAX: 86-10-58607751
michaelT@actintl.com.hk

Hong Kong
Mark Mak
ACT International
Tel: 852-28386298
markm@actintl.com.hk

RFMD®

Compact, Low Loss Switching for High Linearity 2G/3G/4G Applications

1991 • 2011

RFMD offers a family of high-power discrete switch products, which are available in SPDT, SP3T, and SP4T type architectures. These switches are tailored to address coexistence issues in WiFi, BT, GPS, and LTE bands, which require extremely high linearity. These switches have very low current consumption making them ideal for use in battery-powered cellular devices where talk time and standby time are critically important. Other possible applications for these switches include antenna tuning and cellular band switching.

SPECIFICATIONS

	Control Lines	*Freq Range (MHz)*	*Power Handling (dBm)*	*Control Voltage (V)*	*Insertion Loss (dB)*	*Isolation (dB)*	*Switching Speed (uS)*	*IIP2 (dBm)*	*IIP3 (dBm)*	*Package (mm)*	*Mass Production*	*Part Number*
SPDT	1	DC to 3500	36	0 / +1.8	0.3	43	2.00	129	74	2.0 x 2.0 x 0.55	NOW	RF1602
SP3T	2	DC to 3500	36	0 / +1.8	0.4	40	2.00	120	73	2.5 x 2.5 x 0.55	NOW	RF1603A
SP4T	2	DC to 3500	36	0 / +1.8	0.4	40	2.00	120	73	2.5 x 2.5 x 0.55	NOW	RF1604

Order RFMD products online at www.rfmd.com/MWJS1111.

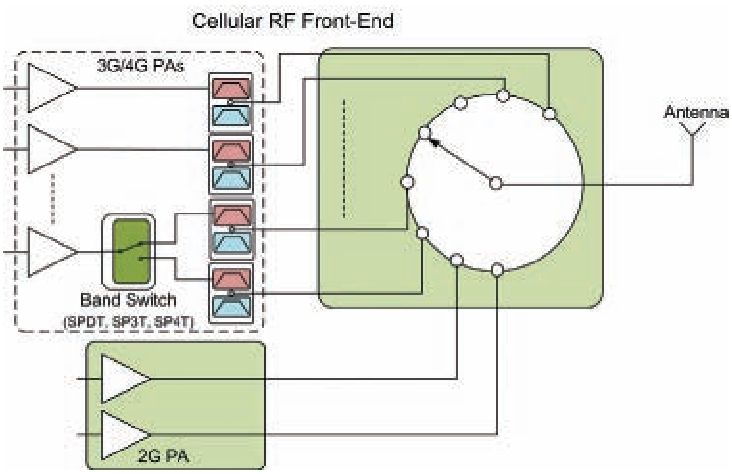

FEATURES

- **Very low insertion loss and high isolation**
- **Excellent linearity performance: IIP2 > 120dBm, TBR > 81dBc**
- **1.8V GPIO compatible**
- **Very low current consumption**
- **Broadband operation across multiple frequency bands and applications**

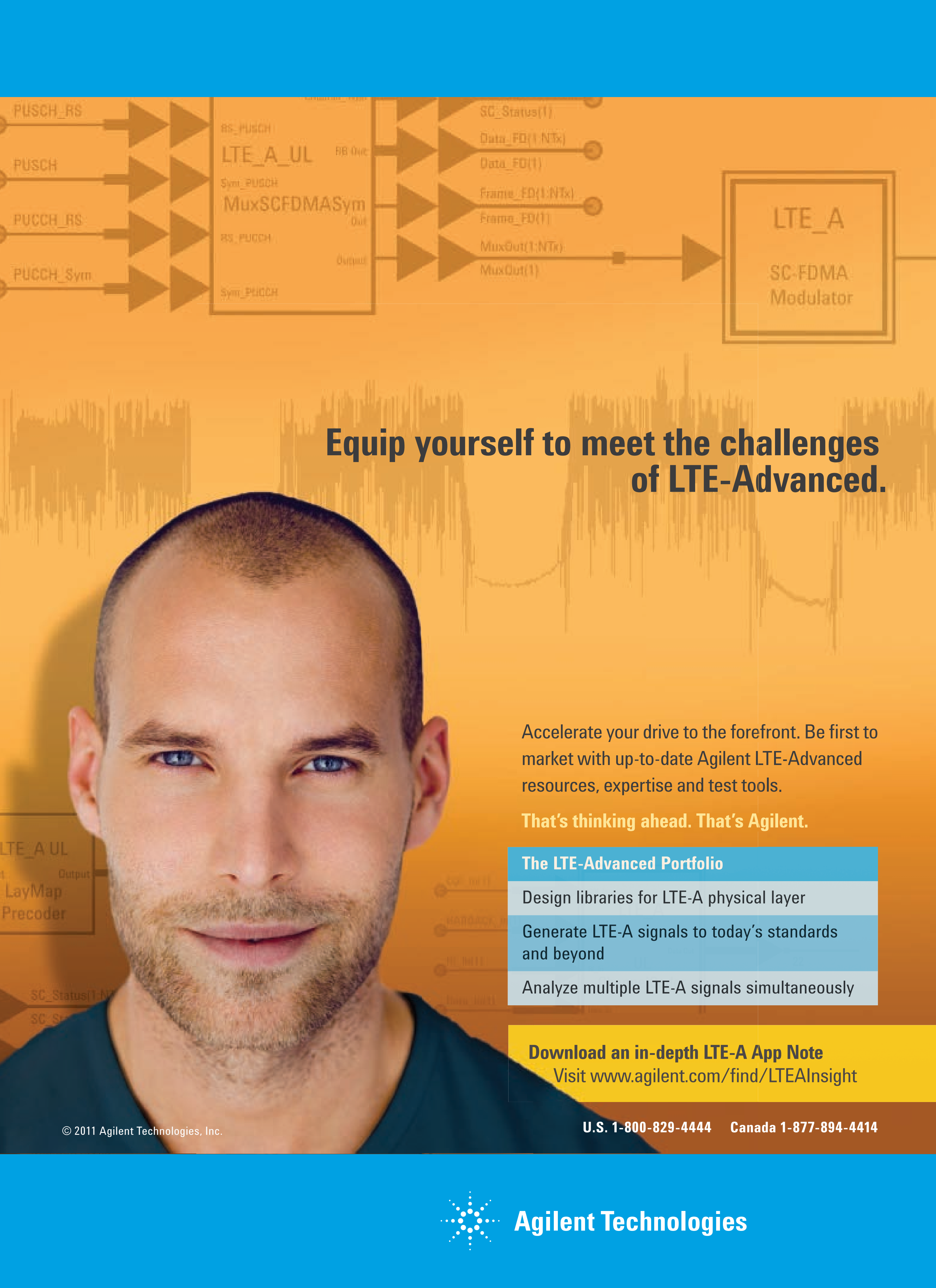
Equip yourself to meet the challenges of LTE-Advanced.
Accelerate your drive to the forefront. Be first to market with up-to-date Agilent LTE-Advanced resources, expertise and test tools.
That's thinking ahead. That's Agilent.
The LTE-Advanced Portfolio
Design libraries for LTE-A physical layer
Generate LTE-A signals to today's standards and beyond
Analyze multiple LTE-A signals simultaneously
Download an in-depth LTE-A App Note
Visit www.agilent.com/find/LTEAInsight
U.S. 1-800-829-4444 Canada 1-877-894-4414
© 2011 Agilent Technologies, Inc.
Agilent Technologies